ChemBioChem

Research Article
doi.org/10.1002/cbic.202200361

Chemistry Europe
European Chemical Societies Publishing

www.chembiochem.org

Special Collection

The Total Synthesis of Glycolipids from *Streptococcus pneumoniae* and a Re-evaluation of Their Immunological Activity**

Seyed Iraj Sadraei,[a] Greg Yousif,[a] S. Maryamdokht Taimoory,[a, b] Maryam Kosar,[a] Samaneh Mehri,[a] Raghd Alolabi,[c] Emmanuel Igbokwe,[a] Jason Toma,[c] Mir Munir A. Rahim,*[c] and John F. Trant*[a]

Invariant natural killer (iNK) T cells, Type I iNKTs, are responsible for the production of pro-inflammatory cytokines which induce a systemic immune response. They are distinctive in possessing an semi-invariant T-cell receptor that recognizes glycolipid antigens presented by CD1d, a protein closely related to the class I major histocompatibility complex, conserved across multiple mammalian species in a class of proteins well-renowned for their high degree of polymorphism. This receptor's first potent identified antigen is the α-galactosylceramide, **KRN7000**, a synthetic glycosphingolipid closely related to those isolated from bacteria that were found on a Japanese marine sponge. A corresponding terrestrial antigen remained unidentified until two specific diacylglycerol-containing glycolipids, reported to activate iNKT cells, were isolated from *Streptococcus pneumoniae*. We report the total synthesis and immunological re-evaluation of these two glycolipids. The compounds are unable to meaningfully activate iNKT cells. Computational modelling shows that these ligands, while being capable of interacting with the CD1d receptor, create a different surface for the binary complex that makes formation of the ternary complex with the iNKT T-cell receptor difficult. Together these results suggest that the reported activity might have been due to an impurity in the original isolated sample and highlights the importance of taking care when reporting biological activity from isolated natural products.

Introduction

The major histocompatibility complex (MHC) proteome, and their associated T-cell receptors are likely the most polymorphic genes in humans, and likewise one of the least conserved systems between mammalian species, meaning that animal models are only of limited value in MHC immunological research due to a high rate of failure in translation to humans in clinical trials.[1] However, there is one notable exception. Both human and mice invariant natural T killer (iNKT) cells express a semi-invariant T cell receptor for the near-completely conserved nonpolymorphic MHC class I-like molecule, CD1d-Vα24-Jα18 in humans,[2] implying that this protein is important for survival.[3] These iNKTs, Type I NKTs, are distinct from the Type II NKTs that express a wider variety of CD1d receptors. This unusual constancy is further emphasized by the ligand recognized by the receptor. Unlike closely related classical MHC class I molecules that recognize peptides, CD1d is specific for exogenous glycosphingolipids.[4] The first highly potent ligand identified was **KRN7000**, **1**, a synthetic model molecule standing in for a series of related glycolipids isolated from a Japanese sea sponge (Figure 1).[5] The molecules were purified from a fraction with highly potent anticancer activity, and upon binding to CD1d activates iNKT cells and induces a potent innate immune system response, leading to the activation of T cell, B cell, dendritic cell and macrophage functions (Figure 1).[6]

KRN7000's unusual mode of action and incredibly potent activity, stimulated a burst of interest in analogues peaking in the first 15 years of the 21st century;[7] the pathway's biological role clearly suggests it represents a defense against an existential threat to survival; consequently, this system has been proposed as potentially manipulatable as a potent, if dangerous, defense against cancers, or systemic pathogenic infections.[8] However, this research left the mystery as to why the mammalian immune system responds to glycolipid antigens isolated from a deep-sea sea sponge, unanswered. A potential solution arose in 2011, when Kinjo and co-workers reported the isolation of two new glycolipid antigens (**2** and **3**) capable of binding to CD1d (Figure 1).[9] The glycolipid antigens were isolated from *S. pneumoniae*, which is the leading cause of neonatal sepsis and meningitis,[10] and until the antibiotic

[a] S. I. Sadraei, G. Yousif, S. M. Taimoory, M. Kosar, S. Mehri, E. Igbokwe, J. F. Trant
Department of Chemistry and Biochemistry
University of Windsor, ON N9B 3P4 Windsor, (Canada)
E-mail: j.trant@uwindsor.ca
[b] S. M. Taimoory
Department of Chemistry, University of Michigan
48109-1055 Ann Arbor, MI (USA)
[c] R. Alolabi, J. Toma, M. M. A. Rahim
Department of Biomedical Sciences
University of Windsor, ON N9B 3P4 Windsor, (Canada)
E-mail: mrahim@uwindsor.ca

[**] *A previous version of this manuscript has been deposited on a preprint server (https://doi.org/10.26434/chemrxiv-2021-nk95v-v2)*

Supporting information for this article is available on the WWW under https://doi.org/10.1002/cbic.202200361

Special Collection *This publication is part of a joint Special Collection with EurJOC and ChemCatChem* on "Carbohydrate Chemistry". Please see our homepage for more articles in the collection.

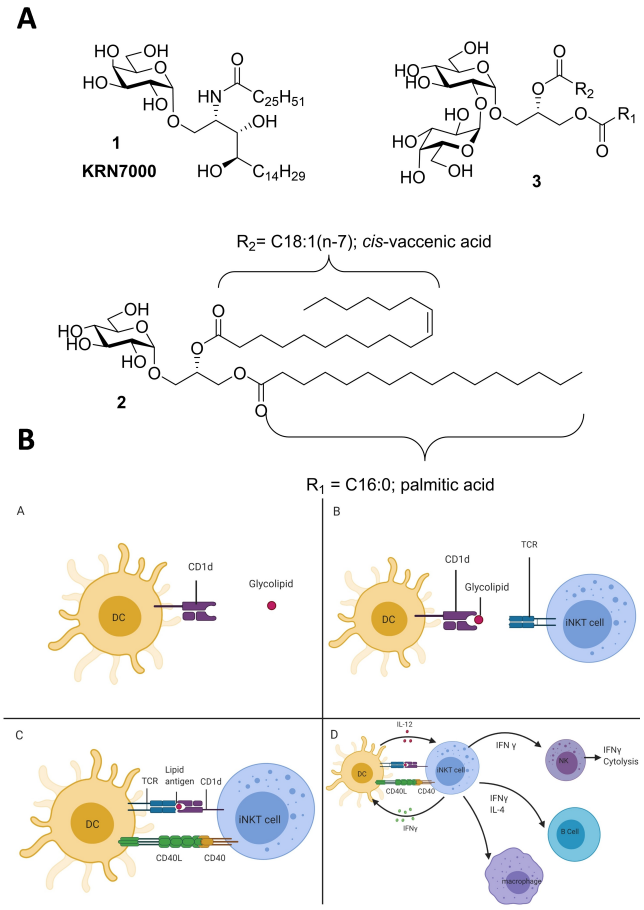

Figure 1. Structure of **KRN7000** (**1**), monosaccharidic glucose diacyl glycerol (**2**), and disaccharidic galactosyl-glucose diacylglycerol (**3**). Cartoon representation of the activation of iNKT cells by the glycolipid antigen presented by the CD1d molecule on a subclass of dendritic cells. A) The dendritic cells express CD1d on their surface that can bind the glycolipid antigen. B) This complex can then bind $V_\alpha14i$ on iNKT cells. C) This then activates the cell, and elicits the recruitment of additional intracellular protein-protein interactions that validate the activation; D) This leads to the production of cytokines by the iNKT that in turn recruits an immune response from NK cells, B cells, and macrophages.

modern era, one of the leading causes of death.[11] The first was identified as consisting of an α-D-glucosylpyranosyl residue O-linked to a diacylglycerol where the primary alcohol was esterified with palmitic acid, and the secondary alcohol with *cis*-vaccenic acid (**2**). The second fraction had the same core, but with a proposed additional α-D-galactosylpyranosyl residue attached at the 2-position of the glucose (**3**).[9] The glycolipid response appeared to be dependent on the inclusion of *cis*-vaccenic acid, which although very common in bacterial and plant samples,[12] is highly unusual in mammals, where the *trans* isomer dominates in mammalian milk.[13]

Both glycolipid antigen isolates activated iNKT cells *in vivo* and *in vitro*. However, these tests were carried out using very small amounts of isolated glycolipids,[9] making it impossible to conclusively ascertain whether the activity was due to these compounds or to some minor impurity. Impurities present in isolated samples are notoriously frustrating in immunological research where very small levels of compounds can have outsized biological effects, this is a known issue for synthetic cholesteryl 6-acylglucosides,[14] where apparently equivalent synthetic batches can have different activity. Kronenberg and co-workers synthesized **2**;[9] however, activity was considerably less for the synthetic version than for the isolated material. This same glycolipid has since been resynthesized once since this original report,[15] and its activity was found to be minimal, and far lower, in relative terms, to **KRN7000** than first reported.[16] This low activity, both in terms of binding affinity to the receptor, and in terms of IL-2 production, was noted by Williams, Rossjohn and co-workers using the broad-spectrum A11B8.2 NKT clone, where it was essentially equivalent to vehicle control, and in the VB8 clone although showing minimal activity, it lagged far behind **KRN7000**.[16b] A related glycolipid associated with flesh-eating bacteria, has been found to stimulate the macrophage inducible C-type lectin; these types of molecules are certainly relevant.[17] Disaccharide **3** was also investigated by Kronenberg and co-workers,[9] but has never been prepared: the authors noted that the activity of the sample might have been due to contamination from the monosaccharide. This is notable as the initial report did not provide incontrovertible proof for the unusual proposed structure. There is only a single other example of a 2-linked Gal-Glc disaccharide coupled to a diacylglycerol reported in the literature, isolated from *Listeria* and involved in cell wall structure.[18] The motif is also proposed as the terminal disaccharide in the polysaccharide-containing Yuccoside C.[19] This particular Gal-Glc disaccharide has never, to the best of our knowledge, been synthesized, let alone conjugated to a diglyceride; however, the glc-glc analogues have been prepared using a different protecting group strategy.[20]

These glycoside diglycerides, incorporating unsaturated fatty acid chains are challenging synthetic targets due to the mutual sensitivity of protecting groups and the esters to standard reagents. The extant synthetic approaches to similar compounds commonly suffer from low efficiency, synthetic flexibility, and stereopurity.[21] Herein we report a simple total synthesis of both *S. pneumoniae* glycolipids, a reevaluation of their biological activity, and an *in silico* investigation of their functional structural biology. We find that they are functionally incapable of activating iNKT cells. We conclude that some of the activity observed in the original report might be attributable to minor impurities present in the evaluated samples, perhaps a glycosphingolipid similar in structure to **KRN7000**.

Result and Discussion

Synthesis of monosaccharidic glucose diacyl glycerol, 2

The synthesis of **2** begins with glucose **4** (Scheme 1), which was converted using standard chemistry to the base-stable β-thiophenol glycoside **5**, lacking a C-2 participating group.[22] The diglyceride acceptor, (*S*)-(+)-Solketal **8**, was synthesized through a modification of Terivedi's strategy to provide the appropriate protected chiral glycerol;[23] the change is the use of lead (IV)

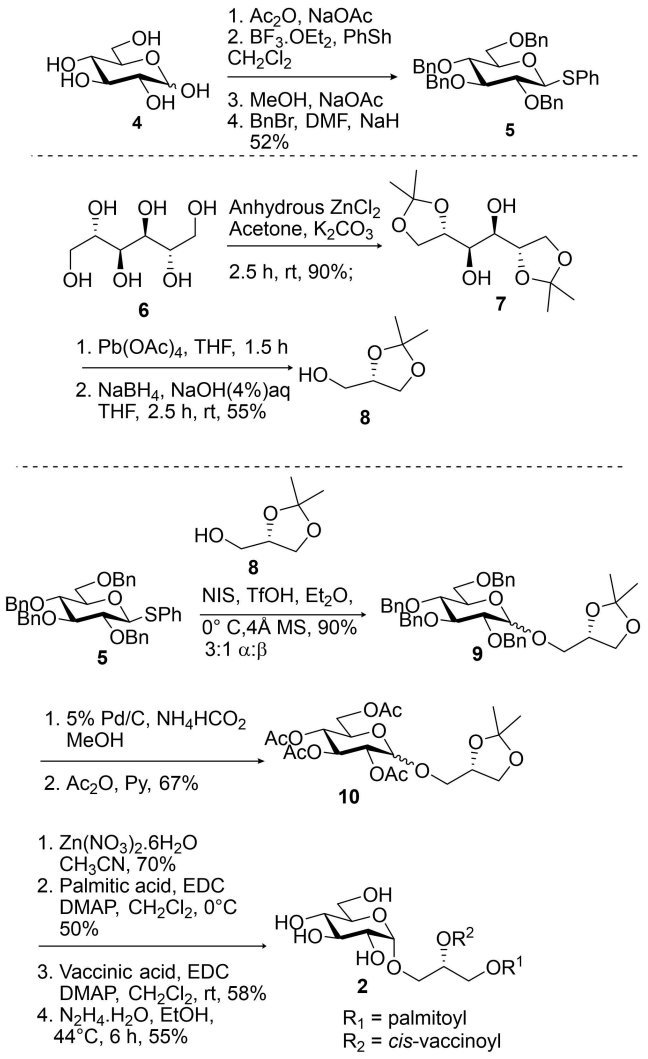

Scheme 1. Synthesis of monosaccharide **2**.

acetate for the oxidative cleavage of the mannitol di-acetonide **7** rather than the reported sodium periodate, which proved irreproducible in our hands.[24]

The glycosylation is superficially simple; however standard α-specific glycosylations failed to provide the desired anomer, all forming the undesired β diastereomer of **9** either exclusively or as the major product (see supporting information, **9a**).[21a,25] This was highly surprising as the glycosylation appears far simpler than most, but perhaps is affected by interference of Lewis acid co-ordination by the proximal ketal on the acceptor, and was especially problematic as the two anomers were completely inseparable by preparative column chromatography. The best ratio achieved was a disappointing 3:1 ratio of α:β anomers of **9** (diethyl ether) in a 90% combined yield of the two stereoisomers, and the mixture of anomers was carried forward with the eventual expectation that separation could be affected in the final step, if necessary, by semi-preparative HPLC. This reaction has proven challenging to others in the past, providing difficult to separate mixtures of the anomers.[26] It is important to note, that under acidic conditions, migration of the isopropylidene and a consequent scrambling of the center has been noted for this solketal;[27] however, this should result in a mixture of enantiomers, generating diastereomers in the glycoconjugate should it occur. Minor glycoside products were removed from the reaction mixture during the column chromatography, but only the two anomers were noted. Our conditions are not dissimilar to others who have also failed to note any such challenge when working with this compound (at a far higher temperature than we employed),[26b] and the sensitivity of the acetal might be overstated in the literature. Improved anomeric ratios could be obtained using intramolecular delivery strategies and tuning of conditions; however, the mixture would likely remain difficult to separate, and we were, when compared with the reports, extremely pleased with the high combined yield of the two anomers, encouraging us to proceed.

Having performed their function, the benzyl groups were replaced with acetates, due to the incompatibility of hydrogenolysis with *cis*-vaccenic acid, to provide fully protected **10** in two steps. Zinc nitrate hexahydrate in acetonitrile selectively hydrolyzed the isopropylidene group of the glyceride to provide the diol.[28] Sequential esterification, relying on the increased reactivity of the primary alcohol over the secondary alcohol, with palmitic acid (at 0 °C) and freshly prepared *cis*-vaccenic acid (at ambient temperature due to a more sluggish reaction)[29] provided the fully protected diglyceride. Following the second esterification, the two anomers surprisingly separated easily by column chromatography as the Rf values, for the first time since **9**, diverged significantly. The reported yields, up until the second esterification, are for the combined mixture of the anomers; the second esterification, with a 58% yield, is reported for the recovery of the pure α-anomer from the mixture, yield from the α-precursor alone was 77%;[30] the β-anomer, was also isolated and recovered at this point. Finally, the desired deprotected glycolipid **2**, was obtained following global deacetylation using hydrazine hydrate in 55% yield.[31] Byproducts in this final step ominously included limited desterification and a small amount of the aglycone. The β-anomer was likewise deprotected to provide pure **2β**.

Synthesis of disaccharidic galactosyl-glucose diacylglycerol, 3

With the monosaccharide in hand, we expected the disaccharide would not prove challenging – "only a matter of marching"[32] – with the only obstacle being efficient access of C-2 free OH glucose **13**. The rest of the synthesis should remain strategically unchanged. Fortunately, we readily solved this single challenge (Scheme 2). As with **2**, glucose was transformed to a fully deprotected thioether, this case ethylthiol-derived **11**. Benzylidene formation followed by acetylation provided **12**. Then, the C-2 hydroxyl was selectively unmasked through Ensley's method of concomitant oxocarbenium formation and acetyl migration to the anomeric position to provide glycosyl acceptor **13** in 40% yield.[33] Multiple glycosylations were investigated to prepare the disaccharide, but simple trichloroacetimidate (TCA) chemistry[34] proved to be

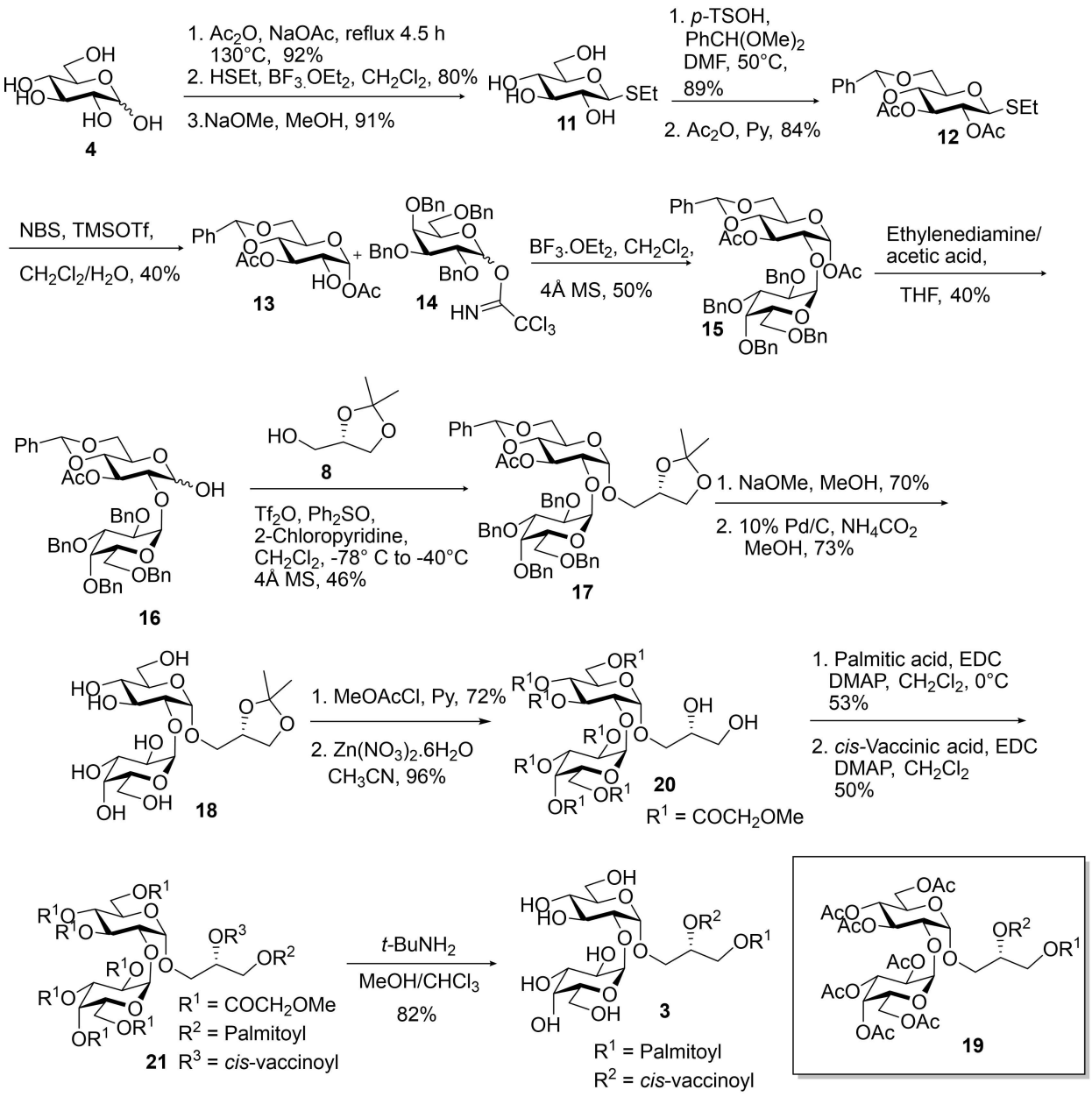

Scheme 2. Synthesis of disaccharide **3**.

sufficiently reliable after a preliminary screen; notably, the reaction was highly sensitive to the stereochemistry of the donor and the Lewis acid. The reaction proceeded only from the α-anomer and using $BF_3{\cdot}OEt_2$. Although we were readily able to generate the β-anomer of the TCA agent in near analytical purity without purification, we were unable to obtain the α anomer in greater than a 1:1 ratio with the β isomer.[34] Freshly distilled TMSOTf did not catalyze the transformation with either anomer even at elevated temperatures and extended reaction times. Test reactions showed that the reaction was facile with almost any other acceptor, and this recalcitrant reactivity is a function of both donor and acceptor.

Anomeric acetates are themselves moderately reactive glycosylation agents;[35] however, continuing the trend of this campaign, **15**, proved to be a reluctant donor for glyceride acceptor **8**, and we were unable to convert the α acetate directly. The chemoselective removal of the acetyl group at anomeric position was accomplished *via* a mixture of ethylene amine and acetic acid in THF after 24 hours,[36] with the mass balance being unreacted starting material that can be resubjected to reaction conditions (longer reaction times started to result in cleavage of the intersaccharidic bond). To limit the step count, we attempted Savage's glycosylation of the free hydroxyl, which was employed for the galactosyl-galactosyl analogue of this current target, using diphenylsulfoxide

activated with triflic anhydride and tri-*tert*-butylpyrimidine as base, but this failed to provide any product.[36] However, increasing the reactivity of the system by using 2-chloropyridine as base proved successful, providing **17**, the core of the glycolipid.[37] The protecting group strategy had been selected to be compatible with the chemistry developed for the monosaccharide. Global deprotection of the carbohydrate protecting groups (without touching the acetonide on the glycerol), proceeded smoothly to **18**.

We then conducted the same sequence used for the monosaccharide to complete the synthesis: peracetylation, acetonide removal, and selective esterifications to generate **19**. However, all attempts to cleave the acetates from the sugars without affecting the esters on the glyceride failed. Reagents variously either cleaved all esters, did not react, were unable to provide selectivity, or cleaved the apparently sensitive intersaccharidic bond. Despite a very significant effort, we were unable to remove the acetates in the presence of the esters without damaging the rest of the molecule. A new approach was required.

Consequently, we employed methoxyacetyl groups that can be cleaved by *tert*-butylamine,[38] as was employed for the monosaccharide by Richardson and co-workers when faced with a similar chemoselective challenge.[15] This is an underappreciated protecting group as the deprotection conditions are highly compatible with a wide variety of different functional groups.[39] Fully deprotected **18** was acylated, the acetonide removed as before, and the esterifications proceeded without difficulty. Fortunately, the *tert*-butylamine, unlike any of the other deacylation reagents tested, was gentle enough to evince the final deprotection to provide **3** in 82% yield.[38c]

iNKT activation ability of the synthetic glycolipids

With **2**, **2β** and **3** in hand, we evaluated their ability to induce production of cytokines by CD1d-restricted iNKT cells. We employed the mouse iNKT cell hybridoma DN32.D3, especially well designed for this experiment as it possesses both the CD1d and the unique conserved, invariant V_α14T cell receptor of iNKT cells, allowing the cells to present antigenic glycolipids and cross-activate each other. This cell line has been used extensively in the past to measure iNKT cell responses, represented by the production of interleukin-2 (IL-2, other cytokines show similar results).[40] These cells produce IL-2 in response to **KRN7000** treatment in a CD1d-dependent manner, making **KRN7000** an excellent positive control. Several other glycolipid formulations have also been shown to induce an immune response from these cell types, including bacterial superantigens (SAgs),[40a] a series of glycolipids from pathogenic bacteria,[41] including the ones synthesized here,[9] and even a multivalent acetal-free,[42] dendron-supported carbohydrate previously reported by us.[40c] Kinjo and co-workers evaluated the immunogenicity of their isolated glycolipids using mouse Va14iNKT cell hybridomas,[9] which are similar to the those used in this study. The isolates showed good elicitation of IL-2 from V_α14*i*NKT cell hybridomas in a CD1d-dependent manner, but no activation of CD1d-reactive non-V_α14*i*NKT cell hybridomas. The original authors then synthesized the monosaccharide and evaluated the immunogenicity of that system (while also confirming the structure and regiochemistry of the ester groups) and demonstrated that it showed similar activity to the isolated monosaccharide.[9] This is not the result we observed here. We observe no meaningful IL-2 response from the DN32.D3 cells towards the synthesized glycolipids at either 100 ng/mL to 1 μg/mL relative to their background response to media (none of the means are statistically significant), while **KRN7000** showed its typical potent activity in inducing IL-2 production by these cells (Figure 2).

This is in stark contrast to the results initially reported by Kronenberg and co-workers,[9] although it is in line with the work of Williams and co-workers. They have shown that the activity of **2** and many derivatives, appears to be potentially dependent on the particular cell clone involved.[16a] This might imply that the mechanism of action may be more complicated than simple binding of the glycolipid to the receptor; note that **1** alone is sufficient to activate the Type I iNKT system regardless of the cell clone. Consequently, we resynthesized fresh batches of the glycolipids, repurified them, and re-evaluated the samples obtaining the same result. We further evaluated the ability of the materials to induce iNKT cells stimulation *in vivo* in C57BL/6 mouse strain. We reasoned that the CD1d-restricted cell line may not provide the full required machinery needed to elicit an iNKT cell response to these modified glycolipids *in vitro*, that a fully intact immune system could provide. This hybridoma is sufficient for antigens that function directly through the CD1d-V_α14T interaction, but it is possible that the antigens function like superantigens and activate the iNKTs indirectly. To this end, we treated groups of mice with 4 μg dose of the glycolipid antigens and **KRN7000** intraperitoneally. Two hours post injection, mice were sacrificed and the percentage of splenic NKT cells expressing IL-4 and IFNγ were determined by intracellular staining and flow cytometry analysis. In our experiments NKT cells were recognized as $NK1.1^+TCR\beta^-$ lymphocytes. Again, **KRN7000** proved a potent stimulator of NKT cells, but none of our synthetic glycolipids showed any significant activity relative to vehicle (Figure 2). Extended *in vivo* stimulation up to 48 hours did not elicit any IL-4 and IFNγ response in iNKT cells against any of the synthetic glycolipids (not shown). These molecules failed to induce IL-4 and IFNγ production by NKT cells *in vivo*. Finally, to ensure that the glycolipid antigens were accessible by dendritic cells (DC) for presentation on CD1d, we used bone marrow-derived DCs pulsed with the glycolipid antigens before adoptively transferring them to CD57B/6 mice to activate NKT cells *in vivo*. Again, the synthetic glycolipid-pulsed DCs failed to elicit any IFNγ production from NKT cells, while **KRN7000**-pulsed DCs were potent activators of NKT cells (Figure 2).

One of the differences between this study and the one by the Kronenberg group is in the iNKT cell hybridomas used to evaluate iNKT cell responses. Our cells (DN32.D3) express both CD1d and the invariant V_α14 T cell receptor, allowing the cells to present antigens and activate each other, while the Kronenberg group used an iNKT cell hybridoma which did not

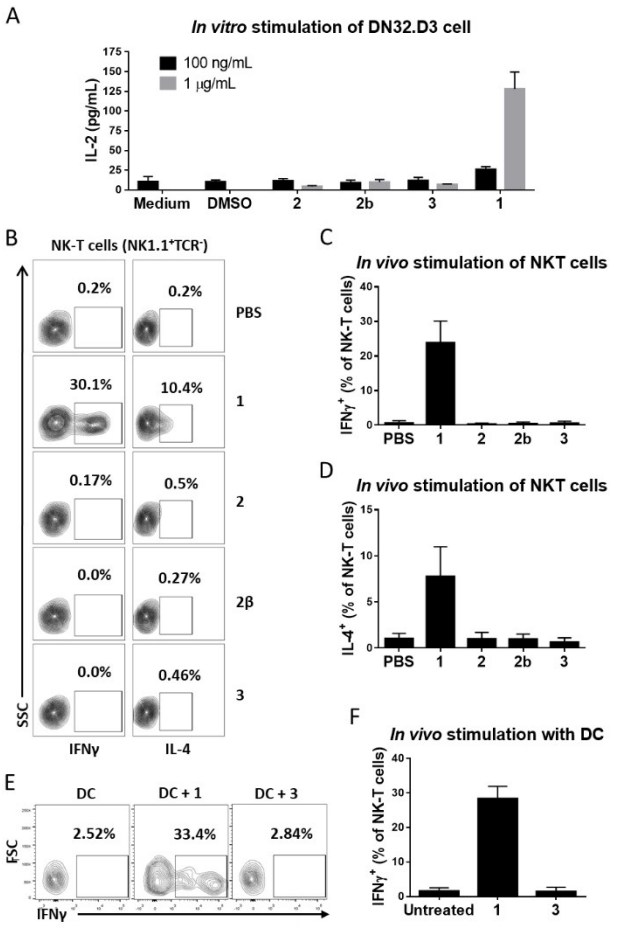

Figure 2. Cytokine production by iNKT cells in response to glycolipid stimulation. A) Elicited IL-2 levels obtained from exposing DN32.D3 cells to the synthesized glycosphingolipids as measured by ELISA. Data represent mean ± standard deviation of triplicate samples. B) Flow cytometry analysis of intracellular IL-4 and IFNγ levels in NKT cells ($NK1.1^+TCR\beta^-$) in the spleens of 8–12 week-old C57BL/6 mice 2 hours after intraperitoneal injection with the indicated agents (4 μg in 200μL PBS/mouse). Percentage of $IL\text{-}4^+$ and $IFN\gamma^+$ cells are indicated for each treatment. Data represent one out of at least 6 mice in each of the treatment groups. C) Quantification of the $IFN\gamma^+$ results from B. D) Quantification of the $IL\text{-}4^+$ results from B. Data represent mean ± standard deviation. E) Flow cytometry analysis of intracellular IFNγ levels in NKT cells in the spleens of C57BL/6 mice 24 hours after adoptive transfer of antigen-pulsed DCs. Percentage of $IFN\gamma^+$ cells are indicated for each treatment. Data represent one out of at least 4–6 mice in each of the treatment groups. F) Quantification of the $IFN\gamma^+$ results from E, representing mean ± standard deviation. **1**, **KRN7000**; **2**, monosaccharidic glucose diacyl glycerol; **2β**, monosaccharidic glucose diacyl glycerol (β-anomer); **3**, disaccharidic galactosyl-glucose diacylglycerol. In none of the experiments were any of **2**, **3**, or **2β** statistically different from the control.

express CD1d, therefore, requiring the use of DC or plate-bound CD1d molecules for presentation of antigenic glycolipids. Using *Il-12*$^{-/-}$ and *Myd88*$^{-/-}$ mice, the Kronenberg group demonstrated that iNKT cell responses in their assays were independent of IL-12 and activation of DC via Toll-like receptors, however, the contribution of other pro-inflammatory cytokines induced by their antigenic preparations cannot be completely ruled out. Alternatively, CD1d-dependant presentation of glycolipids to iNKT cells may require additional processing of the isolated glycolipids by DCs.[9] Our *in vitro* assays are performed in the absence of DCs as antigen presenting cells, therefore, are not subjected to the same factors. Furthermore, our *in vivo* assay in the immunocompetent mice firmly demonstrate that, unlike **KRN7000**, which induced iNKT cell stimulation and cytokine production, our glycolipid preparations did not elicit such a response under similar conditions with the fully intact immune system present. The contribution of glycolipid preparations in the activation of iNKT cells, if any, appears to be mechanistically different than that of **KRN7000**.

The difference between the cell lines used by our research group and that of the Kronenberg group is that our cells had the murine MHC receptors removed, leaving only CD1d.[9] The Kronenberg group's cells still have the other receptors present. Glycolipids do not, as a rule, interact with other MHC receptors, but the possibility remains that this could explain this discrepancy; however, our mice had fully active murine immune systems that are stimulated by **KRN7000**, and would be sensitive to superantigen effects. Not seeing any response makes it less likely that this would be the mechanism of action.

In all our *in vitro* and *in vivo* experiments, **KRN7000**, with a nearly identical solubility profile, and the same proposed mechanism of action, was a potent activator, while these other glycolipids were not. This suggests that the iNKT system did not co-evolve to recognize the presence of these particular glycolipids, this difference in activity could be ascribed to the manner that they interact with the receptor. Other glycolipids, based on glucuronosyl diacylglycerides[43] have also been isolated and show substantial activity.[16b,44]

We know that the CD1d-dependent response to glycolipids is exquisitely sensitive to the structure of the glycolipid antigens (Figure 3). The structure-activity relationship studies conducted on **KRN7000** have been extensive and have repeatedly reiterated that modifications to the structure are often deleterious to its iNKT cell-activating ability.[7] Substitution at C2 as in **22**, is not tolerated except by a sugar; nor are the removal of the hydroxyl groups of the phytosphingosine (i.e. **23**), changes in stereochemistry of the phytosphingosine (**24** and **25**), or replacement of the hydroxyl group by an amine **26**. Introduction of a *Z*-double bond, **27**, also abrogates activity, although the *E* is tolerated. Galactosyl diglycerides like **28**, were initially thought to act on the system, but this glycolipid has now been demonstrated that although an antigen, the effect is likely due to an interaction with Toll-Like receptor TLR4.[45] Likewise, the glucose derivative of **KRN7000** shows very moderate activity. Finally, C-2 substitution of **KRN7000** with an α-D-galactoside is tolerated in the preliminary studies. Together these modifications suggest the glucose derivatives synthesized here could show activity, but perhaps the multiple modifications simply distort the CD1d antigen-bind surface to too great a degree to allow for ternary complex formation with the T-cell receptor. To address this question, we conducted a series of computational analyses.

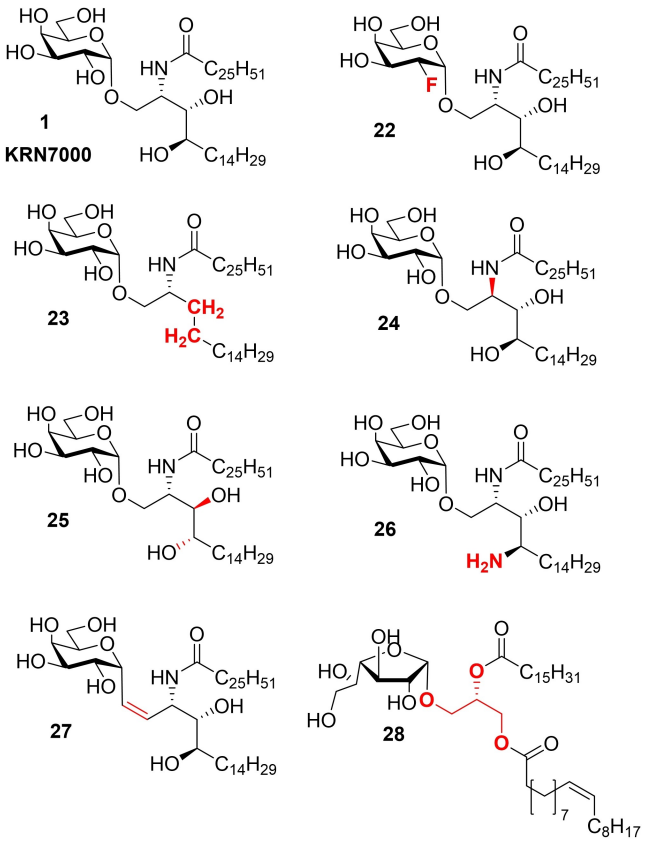

Figure 3. Examples of the modifications to **KRN7000** not tolerated by CD1d.

Computational analysis

Starting with the published crystal structure of the extracellular α1-α3 domains of the CD1d α-chain, and the β_2 microglobulin (β_2M) chain complexed to **KRN7000**, **KRN7000@CD1d** (1ZT4),[46] we solvated the system, then minimized the structure. The resulting conformation remains substantially the same as in the crystal, although we note that the sugar sinks a bit deeper into the pocket in the simulation (Figure 4A). We then deleted **KRN7000** and redocked it, then minimized the structure complexes followed by a 10 ns molecular dynamic simulation to relax the geometry (Figure S2). This matches the crystal structure with high fidelity. The **2@CD1d** and **2@CD1d** structures were obtained by modifying the **KRN7000@CD1d** structure followed by a short molecular dynamics simulation and an optimization of the structure. The extracellular domain of CD1d consists of a *C*-terminal domain, containing two layers of β-sheets (blue and purple, Figure 4), linked to a more structurally complex *N*-terminal binding domain comprising two helices acting as a 'jaw' that hinges shut over a β-sheet floor. This jaw is widest in the center, which determines the position of the carbohydrate of a bound glycolipid, while the long alkyl chains can sprawl into the two large hydrophobic cavities (pockets **A** and **C**) formed between the helices and the β-sheet floor, to the left and right of the jaw's center.

A number of residues position the chains of the binding glycolipid into the pocket, but the polar head group is held in place through a series of hydrogen bond interactions, such as that between the amide of the sphingosine with Thr154 (as either H-bond donor with the glycosidic oxygen atom or a H-bond acceptor with the 2′-NH amide moiety) and Asp151 of the α2-helix (Figure S1); the simulation is consistent with previous examples in the literature.[47] The generated H-bond interactions originated from 2-OH, Thr154, Asp151, and 2′-NH have been shown to play important roles in localizing the polar head group. Similarly, the 3′-OH of the phytosphingosine interacts with Asp80 of the α1-helix, positioning it above the groove. These H-bonding networks, of course, do not exist for the synthetic diglycerides. The main effect this has is that many of these interactions with these rim-residues are taken over by the carbohydrate instead of the phytosphingosine residues. This sinks the sugars deeper into the groove, decreasing their apparent surface (Figure 5), such that they don't extrude from the mouth as far as **KRN7000**.

With **KRN7000**, Trp153 of the α2-helix lies against the more hydrophobic bottom face of galactose, ensuring it orients in the right direction. It is able to do this with **3** as well but as this ligand sits deeper, the torsional bend in the angle is greater, twisting it from coplanar with the groove's floor, to a greater degree. This is further exacerbated as Asp151 then pulls down the sugar though interactions with the C-2 OH of the pendent galactose residue, greatly distorting the positioning of the helix relative to the polar head group compared to **KRN7000**. For **2** the effect is even more drastic as the hexose slides over so that the C3-OH can interact with Asp151, meaning that Trp153 can do little to position the sugar as it is more distant. Finally, Asp80, so central for guiding **KRN7000** into the groove, is now located far from the glycolipids of the diglycerides, and instead of binding to the OH of phytosphingosine, interacts with an adjacent arginine on the α1-helix.

The alkyl chains of these pneumococcal glycolipids do extend down the binding grooves, but they occupy them differently. **KRN7000** has the exceedingly long 26-carbon amide alkyl group that curls around, filling the end of the A-pocket, and sinking deeper into it. This is a large cavity, and it is not satisfied by the far shorter *cis*-vaccenic acid residues. This likely contributes to a lower binding affinity, that although not determined in this, or other, studies, could be partially responsible for the lower observed activity. There are certainly differences in the energy of binding (Figure 5d). We measured the binding affinity of the ligands for the receptor relative to each other, using MM/GBSA calculations from the molecular dynamics simulations (Figure S3), with two separate techniques. The ΔG measures the binding affinity from the native structures of relaxed ligand to the relaxed receptor, with both then compromising to adopt the docked structure. In all cases, this is extremely exothermic and extremely favorable; however, **KRN7000** binds stronger than either of the other two ligands. Our second measurement examines the binding energies when the two species are frozen into their binding conformation ΔG(NS). This "no strain" measurement directly measures the energy gain primarily from desolvation and the formation of the intermolecular interactions. In both cases, **KRN7000** is the far stronger binder. The binding predictions show that the expected binding difference between the disaccharide **3** and **KRN7000** is very minor. Again, there is no significant difference in the need to rearrange to form the complex from the minimal energy conformation of both species; the disaccharide needs the least adjustment to form the binding species. Differences in activation of the iNKT system does not likely arise from differences in binding. All bind well, the difference is likely in how the ligands are presented.

Far more important than binding energy, might be in the exposed surface for ternary complex formation of **TCR∩KRN7000@CD1d** (Figure 5). Plotting the surface of the dimer **KRN7000@CD1d**, shows that it is quite different compared to the other two glycolipids as they sit deeper in the groove as the key interactions are with the sugar itself and not the phytosphingosine residues. This would be partially compensated for if the sugar present was a galactoside as the C4-OH would project out towards solvent, but as this is glucose, we lack this extended volume, shrinking the surface significantly

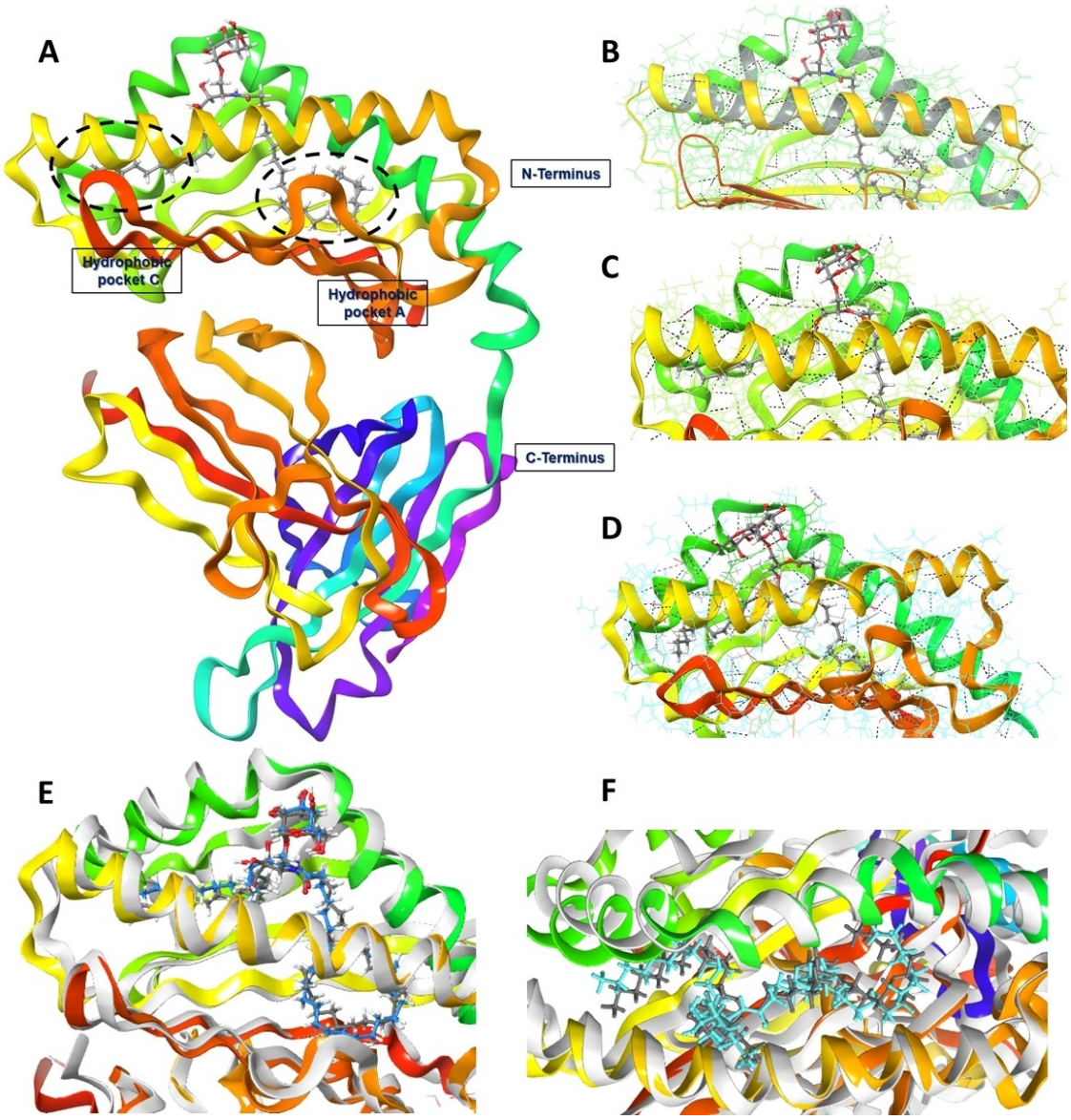

Figure 4. Comparison of the binding modes of the ligands to CD1d. A) Relaxed structure of the complete protein bound to **KRN7000**, **1** (**KRN7000@CD1d**), highlighting the two hydrophobic pockets in the binding groove and the slightly folded down nature of the sugar relative to the crystal structure. B) Focus on the hydrogen bond interactions around the binding site with **1**. C, D) Focus on the hydrogen bond interactions around the binding site with **2** and **3** respectively. E) Side-on view of the superimposition of the modelled **KRN7000@CD1d** onto PDB: 1ZT4.[46]

relative to **KRN7000**. We know that the phytosphingosine residues (specifically the 2′- and 3′-OH) are essential for activity *via* T-cell recognition (Figure 3),[48] and that modification of them weakens the key interactions resulting in loss of activity. We know that the invariant T-cell receptor for CD1d is highly selective for the glycolipid guest in the CD1d receptor, and this selectivity could mean that it is not able to be activated by these residues. To explore this idea, we investigated the ternary complexes computationally (Figure 6).

Minimizing the energy of the **TCR∩KRN7000@CD1d** (Figure 6A, expansion in 6B) shows how the C-4 of the galactose sticks up towards the receptor, pushing the T-cell receptor up and away from the CD1d surface at that point (additional visualizations are provided as Figure S4). It is notable that if the carbohydrate rotated from this point, it would interfere with the required binding surface between the other two partners. This is the preferred interaction mode; exchange of the acyl groups would change the positioning of the sugar, and this would prevent the binding from occurring (as has been noted, swapping the acyl groups on the glycerol doesn't change the pocket preference, so it would change how the sugar sits in the pocket, and it would interfere with ternary complex formation). Glycolipid **2** can sit in the pocket (Figure 6C), but the TCR lowers further onto CD1d. The effect this has on the activation of the receptor is beyond the scope of this work, but it is not the same binding mode, although very similar. One can note that it not only sits deeper in the groove, but it distorts the relative positions of the beta sheets of the two proteins. **KRN7000** sits inside the turn between the two alpha helices of the right side of the binding pocket, while **2** sits over this turn. Similarly, the beta sheet of the TCR in orange interacts directly over the ring of the carbohydrate in **KRN7000**, while we predict it sits over C4 in **2**. This overall drags

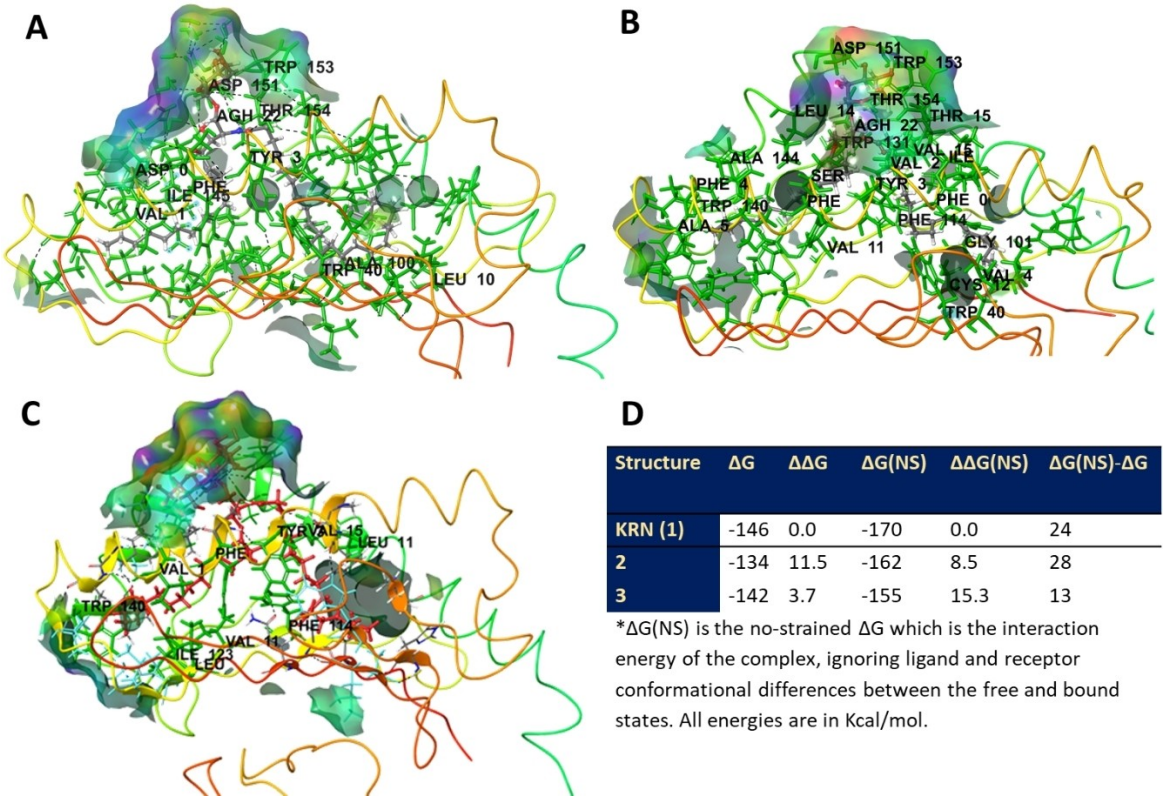

Structure	ΔG	ΔΔG	ΔG(NS)	ΔΔG(NS)	ΔG(NS)-ΔG
KRN (1)	-146	0.0	-170	0.0	24
2	-134	11.5	-162	8.5	28
3	-142	3.7	-155	15.3	13

*ΔG(NS) is the no-strained ΔG which is the interaction energy of the complex, ignoring ligand and receptor conformational differences between the free and bound states. All energies are in Kcal/mol.

Figure 5. Plots of the electrostatic surface of the first hydration sphere around the binding groove of the complexes of A) **KRN7000@CD1d**, B) **2@CD1d**; and C) **3@CD1d**. D) Results of the energy calculations using MMGBSA of the dimer.

the TCR to the right relative to the Cd1d. Glycolipid **3** has the carbohydrate spilling over the alpha helix junction, and distorts the beta sheet of the TCR even further to the right (Figure 6D). This would be expected to affect the TCR activation. These are small difference, but small differences affect the binding of systems. These differences can be quantified; the total binding surface of all systems is relatively similar with the disaccharide being slightly higher than the other two (Figure 6E); however the surface of **KRN7000** involved in receptor binding is larger than for the other two, and the surface of the receptor that binds it is smaller than for the other two; the protein binding pocket is better suited to fit the ligand and can tighten around it. This can also be seen as the total surface are of the system is smallest for **KRN7000@CD1d**. The other two ligands disruption of the surface can be quantified as well as observed qualitatively from the model. It is consistent that the TCR would respond differently to these ligands than it would to **KRN7000**. Perhaps a galactose derivative of **2** or **3** would show more potent activity.

Conclusions

CD1d is an essential component of our intact immune system. It is almost certainly activated by the presence of bacterial glycolipids present in infectious agents such as *S. pneumoniae*. However, the isolated glycolipids **2** and **3** are not responsible for the observed activity. Their synthesis and re-evaluation in this study provides a significant example for the need for the evaluation of synthetic rather than isolated samples as even a very small amount of impurity-undetectable on NMR ($<2\%$)[49] can be responsible for observed activity. The changes to the interaction surface between the **antigen@CD1d** dimer and the T-cell receptor are significant and would modify the interaction. A re-analysis and repurification of these *S. pneumoniae* extracts searching for other known glycolipid activators of CD1d might prove very fruitful to explaining the existence of the invariant iNKT immune defense system.

Experimental Section

General methods and materials for chemical reactions

Solvents were purchased from Caledon Labs (Caledon, Ontario), Sigma-Aldrich (Oakville, Ontario) or VWR Canada (Mississauga, Ontario). Other chemicals were purchased from Sigma-Aldrich, AK Scientific, Oakwood Chemicals, Alfa Aesar or Acros Chemicals and were used without further purification unless otherwise noted. Anhydrous toluene, tetrahydrofuran (THF), diethyl ether and *N*,*N*-dimethylformamide (DMF) were obtained from an Innovative Technology (Newburyport, USA) solvent purification system based on aluminum oxide columns. CH_2Cl_2, pyridine, acetonitrile, *N*,*N*-diisopropylethylamine (DIPEA) and NEt_3 were freshly distilled from CaH_2 prior to use. Purified water was obtained from a Millipore deionization system. All heated reactions were conducted using oil baths on IKA RET Basic stir plates equipped with a P1000 temperature probe. Thin layer chromatography was performed using EMD aluminum-backed silica 60 F254-coated plates and were visualized

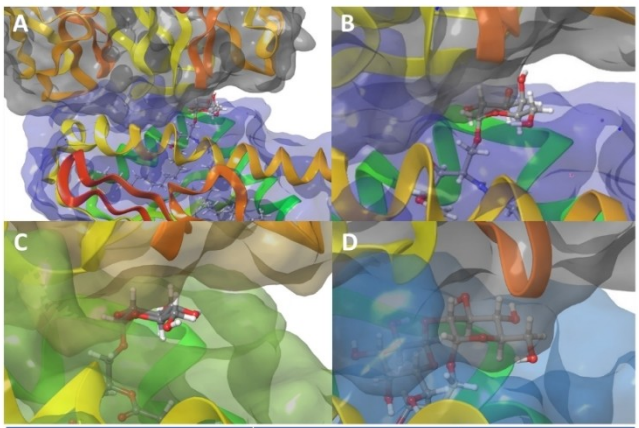

E Surface measured	Area (Å²)		
	KRN7000@CD1d	2@CD1d	3@CD1d
Binding site surface	2729	2726	2834
Ligand-CD1d binding surface	1727	1837	1856
Ligand surface	937	838	888
Total surface of the structure	34696	34835	34741

Figure 6. A plot of the calculated density surfaces of the TCR and CD1d in the ternary complexes in constant color, with the ligand shown in a ball and stick model: A) **TCR∩KRN7000@CD1d**. B) Expansion of the binding site of **TCR∩KRN7000@CD1d**. C) Expansion of the binding site of **TCR∩2@CD1d**. D) Expansion of the binding site of **TCR∩3@CD1d**. E) Table of binding surface areas, defined as follows: Binding site surface is the total top surface of the **antigen@CD1d** outer surface available for binding to the **TCR** bounds were kept the same for all complexes to be directly comparable; Ligand-CD1d binding surface is the surface of the CD1d receptor interacting with the ligand; Ligand surface is the total surface area of the ligand; total structure surface is the surface of the complete **antigen@CD1d** combined outer surface (including the large component of the protein that sits into the membrane).

using either UV-light (254 nm), $KMnO_4$, vanillin, Hanessian's stain, Dragendorff or phosphomolybdic Acid (PMA)'s stain. Preparative TLC was done using glass-backed silica plates (Silicycle) of either 250, 500, 1000 or 2000 μm thickness depending on application. Column chromatography was carried out using standard flash technique with silica (Siliaflash-P60, 230–400 mesh Silicycle) under compressed air pressure. Standard work-up procedure for all reactions undergoing an aqueous wash involved back extraction of every aqueous phase, a drying of the combined organic phases with anhydrous magnesium sulphate, filtration either using vacuum and a sintered-glass frit or through a glass-wool plug using gravity, and concentration under reduced pressure on a rotary evaporator (Buchi or Synthware). ^{1}H NMR spectra were obtained at 300 MHz or 500 MHz, and ^{13}C NMR spectra were obtained at 75 or 125 MHz on Bruker instruments. NMR chemical shifts (δ) are reported in ppm and are calibrated against residual solvent signals of $CHCl_3$ (δ 7.26), DMSO-d5 (δ 2.50), acetone-d5 (δ 2.05), or methanol-d3 (δ 3.31). HRMS were conducted on a Waters XEVO G2-XS TOF instrument with an ASAP probe in CI mode.

Biological experimental protocols

Mice: C57BL/6 mice were purchased from The Jackson Laboratory (Bar Harbor, ME). Mice were maintained in the Central Animal Care Facility in the University of Windsor (Windsor, Ontario) in accordance with the institutional guidelines. All breeding and manipulations performed on mice were reviewed and approved by the Animal Care Committee of the University of Windsor on protocol number 2020-05 issued to Dr. Munir Rahim.

***In vitro* stimulation and IL-2 ELISA**: DN32.D3 cells were generously gifted to us by Dr. Albert Bendelac (Department of Pathology, The University of Chicago). DN23.D3 cells were stimulated *in vitro* with **KRN7000** (αGalCer, Toronto Research Chemicals) and glycolipids **2** or **3** at either 100 nM or 1 μM. The cells were grown in RPMI-1640 medium (Sigma) containing 10% fetal bovine albumin (Sigma), 100 U/mL penicillin (Gibco), 10 μg/mL streptomycin (Gibco), non-essential amino acids (HyClone), 1 mM sodium pyruvate (Gibco), 10 mM HEPES (Gibco) and 55 μM β-mercaptoethanol (Gibco). Approximately, 10^5 cells were incubated with 100 ng/mL and 1 μg/mL of KRN7000 or our glycolipid formulations in a 96-well plate at 37 °C and 5% CO_2 environment for 24 hours. IL-2 in the culture supernatant was measured by enzyme-linked immunosorbent assay (ELISA) following the manufacturer's instructions (mouse IL-2 ELISA kit, Invitrogen). All experiments were repeated in triplicate on separate days; data presented is the mean of the three measurements, with the error reported as standard deviation.

Antigen-pulsed bone marrow-derived dendritic cells (BM-DC): To prepare BM-DCs, 2×10^6 bone marrow leukocytes were incubated in 10 mL or RPMI (Sigma) medium supplemented with 10% fetal bovine albumin (Gibco), 100 U/mL penicillin (Gibco), 100 μg/mL streptomycin (Gibco), 50 μM 2-mercaptoethanol (Gibco), and 200 U/mL granulocyte monocyte-colony stimulating factor (GM-CSF, PeproTech). On day 3, an additional 10 mL of medium containing 200 U/mL GM-CSF was added to the cells. On day 6, half of the culture medium was removed and centrifuged at 500 xg for 5 min to collect the cells. Cells were resuspended in 10 mL of medium containing 200 U/mL GM-CSF and added back to the plate. On day 8, cells were harvested and counted. Approximately, 2×10^6 cells were incubated with 1 μg/mL **KRN7000** or 10 μg/mL glycolipid **3**, or left untreated in 3 mL medium containing 200 U/mL GM-CSF in a 6-well plate for 24 hours. Cells were then harvested, washed three times with phosphate buffered saline (PBS), counted, and resuspended in sterile PBS at 2.5×10^6 cells/mL.

***In vivo* NK-T cell stimulation and cytokine measurements**: *In vivo* stimulation of NK-T cells was performed by intraperitoneal injections of the glycolipid antigens or by intravenous injections of antigen-pulsed BMDC. KRN7000 (αGalCer) or our glycolipid formulations (4 μg) were injected into groups (2–3 mice) of 8–12 week-old C57BL/6 mice intraperitoneally in 200 μL phosphate buffered saline (PBS) for 2 hours or 48 hours. Control mice received only PBS injections. BM-DCs (5×10^5 cells in 200 μL volume) were injected intravenously through the tail vein of 8–12 week-old C57BL/6 mice for 24 hours. Mice were then euthanized and spleens were harvested. Spleens were mechanically dissociated and splenocytes were collected in PBS. Red blood cells were lysed using 2 M ACK (Ammonium-Chloride-Potassium) lysis buffer, and live cells were counted. Approximately, 10^6 splenocytes were incubated with protein transport inhibitors, 2 μM monensin (BioLegend) and 5 μg/mL brefaldin A (BioLegend), in a 96-well plate in 200 μL of RPMI-1640 medium (Sigma) containing 10% fetal bovine albumin (Sigma), 100 U/mL penicillin (Gibco), 100 μg/mL streptomycin (Gibco). Cells were stained with fluorochrome-conjugated antibodies for flow cytometry analysis. Briefly, cells were incubated with anti-CD16/32 Fc-block antibody (clone 93, BioLegend) for 10 min followed by incubation with AlexaFluor700- or PE/Dazzle 594-conjugated anti-NK1.1 antibody (clone PK136, BioLegend), FITC-conjugated anti-CD3 antibody (clone 17 A2, BioLegend), and fixable viability dye (Zombie-NIR, BioLegend) in FACS buffer (PBS, 0.5% bovine serum albumin, and 0.02% NaN_3) for 20 min at 4 °C in the dark. For intracellular cytokine staining, cells were then washed with FACS buffer, fixed and permeabilized with Fixation and Perm Wash buffers (BioLegend), and stained with PE-conjugated anti-IFN-γ (clone XMG1.2, BioLegend) and APC-conjugated anti-IL-4 antibody (clone 11B11, BioLegend) antibodies following the manufac-

turer's instructions. Cells were analyzed with a BD LSR Fortessa™ X-20 flow cytometer (Becton, Dickinson and Company).

Computational chemistry protocols

Rigid receptor docking was initially performed on the optimized structure of ligand using the Glide module of Schrodinger package for which a series of hierarchical filters to search for possible conformational, orientational and positional space of the docked ligands as well as possible locations of the ligand in the binding-site region of a receptor were screened. The scoring function applied in this study was Glide XP. To obtain the highest-quality docking results, the receptor and ligand structures were initially prepared by the Protein Preparation Wizard and LigPrep. In this rigid docking study, the receptor structure was fixed while the ligand was docked into the binding site. Thus, the flexibility of the protein during this rigid molecular docking was not considered. The best docking poses of the ligand within the RMSDs range of 1.0 to 15 Å with reference to the native position was further studied for subsequent MD simulation using the Desmond module. The X-ray binary structures of the human-CD1d/α-GalCer complex reported by Koch *et al.*[46] and Zajonc *et al.*[50] were taken for MD simulation to probe the structural behavior of the polar head group as well as the conformational aspects of the tails during the modelling. The ligand force fields parameters were taken from the general Amber force field (GAFF), whereas AM1 ESP atomic partial charges were assigned to the ligands. The structural preparation and minimization of the binary X-ray structures was performed using the Schrodinger software with the OPLS force field. The prepared and refined structures were then solvated in a truncated octahedral periodic box of TIP4P water molecules with each side at 15 Å. After neutralization of the entire system with counter ions, the energy of the water molecules was further minimized with 1000 steps of steepest descent followed by 3500 steps of conjugate gradient minimization. The molecular dynamics simulations started with a 1 fs integration time step; the complexes' structure was relaxed for 10 ps. Next, the temperature of the relaxed system was then equilibrated at 300 K via 20 ps of MD by 2 fs time steps. A constant volume periodic boundary was arranged to equilibrate the temperature of the complex using the Langevin dynamics applying a collision frequency of 10 ps^{-1} with a velocity limit of 5 temperature units. During the equilibration step, the binary complex in the solvent box was confined to the initial coordinates with a weak force constant of 10 kcal mol^{-1} $Å^{-1}$. The generated coordinates after 20 ps was then applied to do 1 ns molecular dynamics using 2 fs time steps, with temperature being fixed at 300 K using the Langevin dynamics a collision frequency of 1 ps^{-1} and a velocity limit of 20 temperature units. The pressure of the solvated system was then equilibrated at 1 bar at a specified density in a constant pressure periodic boundary by an isotropic pressure scaling method using a pressure relaxation time of 2 ps with the time step of the 2 fs with a cut-off of 9 Å for the non-bonded interaction.

MM/GBSA methods: Using the MM/GBSA method, the free energy ligand, receptor, and complex is decomposed into a gas-phase MM-based energy, polar, and nonpolar solvation energies, and an entropy term.[51] Prime MM-GBSA is a physics-based module which computes the force field energies in implicit solvent of both bound and unbound molecules in the binding process. The MM-GBSA binding energy is modelled applying eq 1, where E is energy involving terms such as protein–ligand van der Waals contacts, electrostatic interactions, ligand de-solvation, and internal strain (ligand and protein) energies.[52]

$$\Delta G_{Binding} = E_{Complex} - E_{Protein} - E_{Ligand} \quad (1)$$

It is important to note that in this MM-GBSA method the entropy terms related to the ligand or protein, does not incorporated. But solvent entropy is included in the VSGB2.1 model of energy, same as the other Generalized Born (GB) and Poison–Boltzmann (PB) continuum solvent models.[52]

In this study, MM/GBSA calculations were carried out for each of the three complexes of monosaccharide, disaccharide and KRN using the OPLS3e force field and the VSGB2.1 solvation model in the Schrodinger package, that is a surface-generalized Born model with a variable dielectric correction and incorporates the effects of hydrogen bonding, π–π interactions, self-contact corrections, and hydrophobic packing in Prime version 3.4.[53]

Specific experimental protocols

***O*-Hexadecanoyl-2-*O*-*cis*-octadec-12-enoyl-3-*O*-(α-D–glucopyranosyl)-sn-glycerol (2)**: Compound **10c** (0.11 g, 0.12 mmol) was dissolved in EtOH (2.5 mL) and $N_2H_4 \cdot H_2O$ 35% (0.3 mL) was added and refluxed at 40 °C for 4.5 h. EtOH was then evaporated under reduced pressure and H_2O (20 mL) was added. The aqueous phase was extracted with CH_2Cl_2 (4×20 mL) and organic phase was washed with brine (40 mL). The organic phase was dried, filtered, and concentrated under reduced pressure. The crude product was dissolved in ethyl acetate and passed through a silica gel column to produce **2**, title compound as a colorless liquid (0.05 g, 55% yield). Rf = 0.28. 98 : 2 EtOAc/MeOH. ^{1}H NMR (500 MHz, MeOD) δ_{ppm} 5.37 (t, J = 5.10, 2H), 5.28 (m, 1H), 4.8 (t, J = 3.15, 1H), 4.45 (m, 1H), 4.2 (m, 1H), 3.87 (dd, J = 10.78, 5.79, 1H), 3.79 (ddd, J = 2.46, 5.25, 11.83, 1H), 3.51–3.72 (m, 4H), 3.39 (m, 1H), 3.31, (m, 1H), 2.33 (m, 4H), 2.04 (m, 4H), 1.62 (m, 4H), 1.32 (s, 44H), 0.91 (td, J = 1.95, 6.82, 6H). ^{1}H NMR (500 MHz d_6-Me_2SO-$CDCl_3$ (5 : 1, v/v) δ_{ppm} 5.37–5.20 (m, 2H), 5.18–5.07 (m, 1H), 4.90–4.81 (m, 1H), 4.81–4.73 (m, 1H), 4.70–4.58 (m, 2H), 4.44–4.35 (m, 1H), 4.35–4.26 (m, 1H), 4.18–4.08 (m, 1H), 3.77–3.65 (m, 1H), 3.63–3.55 (m, 1H), 3.53–3.43 (m, 2H), 3.43–3.33 (m, 2H), 3.22–3.16 (m, 1H), 3.13–3.06 (m, 1H), 2.28–2.22 (m, 4H), 2.00–1.93 (m, 4H), 1.55–1.45 (m, 4H), 1.32–1.15 (m, 44H), 0.85 (dd, *J* = 7.38, 6.65 Hz, 6H). Spectral data is consistent with the literature.[9,54]

1-*O*-Hexadecanoyl-2-*O*-*cis*-octadec-12-enoyl-3-*O*-(β-D–glucopyranosyl)-sn-glycerol (2b): Compound **10d** (85 mg, 0.09 mmol) was dissolved in EtOH (2.5 mL) and $N_2H_4 \cdot H_2O$ 35% (0.3 mL) was added and refluxed at 40 °C for 2.5 h. EtOH was then evaporated under reduced pressure and H_2O (20 mL) was added. The aqueous phase was extracted with CH_2Cl_2 (4×20 mL) and organic phase was washed with brine (40 mL). The organic phase was dried, filtered, and concentrated under reduced pressure. The crude product was dissolved in ethyl acetate and passed through a silica gel column to produce **10e**, title compound as a colorless liquid (48 mg, 53% yield). Rf = 0.29 (98% EtOAc, 2% MeOH). ^{1}H NMR (500 MHz, $CDCl_3$) δ_{ppm} 5.49–5.30 (m, 1H), 5.30–5.21 (m, 1H), 4.94 (ddd, J = 26.58, 19.21, 1.34 Hz, 1H), 4.74–4.47 (m, 1H), 4.44–4.34 (m, 2H), 4.31 (d, J = 7.43 Hz, 2H), 4.16 (ddd, J = 18.57, 12.05, 6.57 Hz, 1H), 3.97–3.86 (m, 1H), 3.83 (s, 2H), 3.75–3.65 (m, 2H), 3.63–3.47 (m, 3H), 3.37 (t, J = 7.97, 7.97 Hz, 1H), 3.30 (d, J = 5.75 Hz, 1H), 2.38–2.20 (m, 4H), 2.04–1.96 (m, 3H), 1.66–1.51 (m, 4H), 1.37–1.13 (m, 44H), 0.87 (t, J = 6.91, 6.91 Hz, 6H). Spectral data is consistent with the literature.[55]

(*Z*)-(*S*)-1-(((2*S*,3*R*,4*S*,5*S*,6*R*)-4,5-Dihydroxy-6-(hydroxymethyl)-3-(((2*R*,3*R*,4*S*,5*R*,6*R*)-3,4,5-trihydroxy-6-(hydroxymethyl)tetrahydro-2*H*-pyran-2-yl)oxy)tetrahydro-2*H*-pyran-2-yl)oxy)-3-(palmitoyloxy)propan-2-yl octadec-6-enoate (3): Compound **21** (6.60 mg, 0.005 mmol) was dissolved in *t*-butylamine (0.05 mL, 0.43 mmol), $CHCl_3$ (0.09 mL) and MeOH (0.30 mL), and stirred at 0 °C for 10 min. The reaction mixture then warmed to room temperature and stirred for 2 h. The solvents were evaporated under high

vacuum. The crude product was dissolved in methanol/ethyl acetate (1:9) and passed through a silica gel column to produce **3**, title compound as a colorless liquid (3.50 mg, 82% yield). Rf = 0.2. 1:9 EtOAc/MeOH. ^{1}H NMR (500 MHz, MeOD) δ_{ppm} 5.39–5.31 (m, 2H), 5.29–5.20 (m, 1H), 5.04 (dd, *J* = 16.54, 3.66 Hz, 2H), 4.58 (s, 1H), 4.49 (dd, *J* = 12.20, 2.89 Hz, 1H), 4.26–4.20 (m, 1H), 4.13–4.07 (m, 1H), 3.94–3.85 (m, 2H), 3.83–3.61 (m, 8H), 3.61–3.56 (m, 2H), 3.40–3.33 (m, 2H), 2.34 (td, *J* = 14.23, 7.24, 7.24 Hz, 4H), 2.09–2.00 (m, 4H), 1.67–1.55 (m, 4H), 1.36–1.26 (m, 44H), 0.93–0.87 (m, 6H). (Five peaks are under solvent peaks) ^{13}C NMR (125 MHz, MeOD) δ_{ppm} 174.7, 173.4, 96.8, 96.3, 76.3, 72.5, 72.0, 71.2, 70.1, 70.0, 70.0, 69.7, 69.6, 68.9, 65.7, 65.3, 62.6, 61.5, 61.2, 33.8, 33.6, 31.7, 29.4, 28.8, 26.8, 24.7, 13.1. **EI-MS *m/z*** calcd for $C_{49}H_{90}O_{15}$ 918.6280 $[M]^+$; $C_{49}H_{90}O_{15}Na$ $[M+Na]^+$: 941.6177. Found: 941.6180.

1,2,5,6-Di–isopropyliidene-D–mannitol (7): Acetone (50 mL) was saturated with anhydrous $ZnCl_2$ (10.0 g, 76.8 mmol) and the milky solution was allowed to settle down. Solution was cannulated under nitrogen to a round bottom flask containing D-mannitol (5.00 g, 27.4 mmol). The reaction mixture was stirred for 2.5 h at room temperature and saturated K_2CO_3 (40 mL) was then added. The reaction mixture was stirred at room temperature for 0.5 h before being filtered. The filtrate and the residue extracted with CH_2Cl_2 (3×50 mL) and the organic phase was dried, filtered, and concentrated under reduced pressure. The crude product was recrystallized from 9:1 hexanes/CH_2Cl_2 to produce **7**, title compound as a white solid (6.00 g, 90% yield). Rf = 0.37. 1:7 EtOAc/hexanes. ^{1}H NMR (300 MHz, $CDCl_3$) δ_{ppm} 4.19 (q, J = 6.03, 2H), 4.13 (t, J = 8.33, 2H), 4.0 (d, J = 5.58, 1H), 3.97 (d, J = 5.6, 1H), 3.76 (t, J = 6.17, 2H), 2.72 (d, J = 6.66, 2H), (s, 6H), 1.35 (s, 6H). Spectral data is consistent with the literature.[56]

(*S*)-(+)-1,2-Isopropylideneglycerol or (*S*)-(+)-solketal (8): Compound **7** (10.0 g, 38.1 mmol) was dissolved in THF (150 mL) and lead (IV) acetate (16.8 g, 38.1 mmol) was added. The reaction was stirred for 30 minutes at 0 °C and 1 h at room temperature. The reaction mixture was filtered and $NaBH_4$ (2.88 g, 76.2 mmol) was added in 4% NaOH (aq.) to the filtrate. The reaction mixture was stirred at 0°C for 30 minutes and then 2 h at room temperature. The reaction mixture was quenched with NH_4Cl, concentrated under reduced pressure, and diluted with CH_2Cl_2 (250 mL). The aqueous phase was extracted with CH_2Cl_2 (3×150 mL) and the organic phase was dried, filtered, and concentrated under reduced pressure. The crude product was dissolved in hexanes/ethyl acetate (3:1) and passed through a silica gel column to produce **8**, title compound as a colorless liquid (2.80 g 55% yield). Rf = 0.4. 3:7 EtOAc/hexanes. ^{1}H NMR (300 MHz, $CDCl_3$) δ_{ppm} 4.20–4.27 (m, 1H), 4.05 (t, J = 8.28, 1H), 3.81 (dd, J = 6.53, 8.17, 1H), 3.71 (d, J = 3.81, 1H), 3.60 (dd, J = 4.79, 11.70, 1H), 1.43 (s, 3H), 1.37 (s, 3H). Spectral data is consistent with the literature.[56]

(2*R*)-1-*O*-(2,3,4,6-Tetra-*O*-benzyl-α-D–glucopyranosyl)-2,3-*O*-isopropylideneglycerol (9): Compound **5** (4.80 g, 7.60 mmol), (*S*)-(+)-Solketal **8** (1.0 g, 7.60 mmol) and activated 5 Å MS stirred in Et_2O (100 mL) for 0.5 h and cooled to −40 °C then TfOH (0.14 mL, 16.2 mmol), and NIS (1.71 g, 7.60 mmol) were added. The reaction mixture was then stirred for 2 h and then passed through Celite upon completion. The reaction was diluted with CH_2Cl_2 (100 mL) and the organic phase was washed with $Na_2S_2O_3$ (100 mL), saturated aqueous $NaHCO_3$ (100 mL) and brine (100 mL), then concentrated. The crude product was dissolved in toluene/ethyl acetate (9:1) and passed through a silica gel column to produce **9**, the title compound as a colorless liquid (4.50 g, 90% yield). Rf = 0.29. 3:7 EtOAc/hexanes. Mixtures of α and β: ^{1}H NMR (300 MHz, $CDCl_3$) δ_{ppm} 7.41–7.27 (m, 14H), 7.25–7.08 (m, 6H), 5.05–4.90 (m, 1H), 4.90–4.71 (m, 3H), 4.71–4.62 (m, 1H), 4.62–4.55 (m, 1H), 4.48 (d, J = 11.64 Hz, 2H), 4.40–4.28 (m, 1H), 4.12–4.03 (m, 1H), 4.03–3.86 (m, 1H), 3.84–3.35 (m, 9H), 1.43 (s, 3H), 1.37 (s, 3H). Spectral data is consistent with the literature.[57]

(2*R*)-1-*O*-(2,3,4,6-Tetra-*O*-benzyl-β-D–glucopyranosyl)-2,3-*O*-isopropylideneglycerol (9a): The fully benzylated glycosyl donor chloride (160 mg, 0.28 mmol), 2–6-di-*tert*-butylpyrimidine (180 mg, 0.95 mmol), molecular sieves and (*S*)-(+)-Solketal **8** (50 mg, 0.378 mmol) were stirred in anhydrous CH_2Cl_2 (2 mL) under nitrogen. AgOTf (160 mg, 0.60 mmol) was added to the reaction mixture. After the disappearance of starting material, Bu_4NBr (120 mg) and saturated aqueous $NaHCO_3$ (10 mL) were added, and the mixture was filtered through a pad of Celite, diluted with CH_2Cl_2 (30 mL) and the mixture was washed with water (30×2 mL), and the organic phase was dried, filtered, and concentrated under reduced pressure. The crude product was dissolved in hexanes/ethyl acetate (3:1) and passed through a silica gel column to produce **9a**, title compound as a colorless liquid (100 mg, 54% yield). ^{1}H NMR (300 MHz, $CDCl_3$) δ_{ppm} 7.29 (m, 18H), 7.18 (m, 2H), 5.02–4.25 (m, 10H), 4.09 (m, 2H), 3.84 (dd, J = 5.99, 8.28, 1H), 3.71 (m, 2H), 3.62 (m, 3H), 3.46 (t, J = 7.93, 2H), 1.42 (s, 3H), 1.37 (s, 3H). Spectral data is consistent with the literature.[57a]

(2*R*)-1-*O*-(α-D-Glucopyranosyl)-2,3-*O*-isopropylideneglycerol (9b): To a solution of compound **9** (3.50 g, 5.32 mmol) MeOH (200 mL), Palladium on Carbon Pd/C (21.0 g, 99.0 mmol) and ammonium formate (6.40 g, 102 mmol) were added and refluxed at 70 °C for 5 h. After cooling to room temperature, the reaction mixture was passed through a Celite pad and washed with MeOH (100 mL). The solvent was evaporated and then co-evaporated with chloroform to return **9b**, the title compound as a colorless liquid compound (1.40 g, 89% yield). Rf = 0.25. 95:5 EtOAc/MeOH. Mixtures of α and β anomers recovered: ^{1}H NMR (300 MHz, MeOD) 5.16–4.97 (m, 1H), 4.82–4.75 (m, 2H), 4.38–4.19 (m, 1H), 4.15–3.97 (m, 1H), 3.94–3.40 (m, 8H), 3.39–3.31 (m, 1H), 3.16 (d, J = 7.85 Hz, 1H), 1.85 (s, 1H), 1.36 (s, 3H), 1.29 (s, 3H). Spectral data is consistent with the literature.[20b,57b]

(2*R*)-1-*O*-(α-D-2,3,4,6-Tetra-*O*-acetyl-glucopyranosyl)-2,3-*O*-isopropylideneglycerol (10): Compound **9b** (1.80 g, 6.12 mmol) was added to pyridine (13 mL) and acetic anhydride (7 mL) at 0 °C, under nitrogen. The reaction was stirred overnight for 12 h and then poured into a beaker containing ice water (100 mL), and then CH_2Cl_2 (100 mL) was added and the aqueous and organic phase were separated. The organic phase was washed once with $CuSO_4$ aq. (2×50 mL), saturated aqueous $NaHCO_3$ (50 mL) and water CH_2Cl_2 (50 mL). The organic phase was dried, filtered, and concentrated under reduced pressure. The crude product was dissolved in hexanes/ethyl acetate (7:3) and passed through a silica gel column to produce **10**, the colorless liquid compound (1.90 g, 67% yield). Rf = 0.45. 3:7 EtOAc/hexanes. Mixtures of α and β anomers recovered: ^{1}H NMR (300 MHz, $CDCl_3$) δ_{ppm} 5.49 (t, J = 9.83, 1H), 5.26–4.95 (m, 2H), 4.89–4.81 (m, 1H), 4.27–4.22 (m, 2H), 4.19–3.98 (m, 3H), 3.82- 3.61 (m, 2H), 3.52–3.44 (m, 1H), 2.06 (acetate singlets, 12H), 1.42 (s, 3H), 1.37 (s, 3H). Spectral data is consistent with the literature.[58]

3-*O*-(α-D-2,3,4,6-Tetra-*O*-acetyl-glucopyranosyl)-sn-glycerol (10a): To a solution of compound **10** (1.80 g, 3.90 mmol) in acetonitrile (18 mL), $Zn(NO_3)_2.6H_2O$ (5.80 g, 19.5 mmol) was added. The mixture was stirred for 6 h at 50 °C, and the solvent was then evaporated under reduced pressure. The reaction mixture diluted with CH_2Cl_2 (150 mL) and water (100 mL) added, and the organic phase was washed with water (2×100 mL) and brine (100 mL). The organic phase was dried, filtered, and concentrated under reduced pressure. The crude product was dissolved in hexanes/ethyl acetate (5:1) and passed through a silica gel column to produce **10a**, the colorless liquid compound (1.20 g, 70% yield). Rf = 0.3. EtOAc. of α and β anomers recovered: ^{1}H NMR (500 MHz, $CDCl_3$) δ_{ppm} 5.55–5.40

(m, 1H), 5.15–5.00 (m, 2H), 5.00–4.87 (m, 1H), 4.32–4.17 (m, 1H), 4.17–4.04 (m, 2H), 4.01–3.59 (m, 6H), 2.63–2.54 (m, 1H), 2.11 (s, 3H), 2.08 (s, 3H), 2.05 (s, 3H), 2.03 (s, 3H). Spectral data is consistent with the literature.[59]

1-*O*-Hexadecanoyl-3-*O*-(*α*-D-2,3,4,6-tetra-*O*-acetyl-glucopyranosyl)-sn-glycerol (10b): To a solution of compound **10a** (1.20 g, 2.76 mmol) in anhydrous CH_2Cl_2 (50 mL) under nitrogen, palmitic acid (0.72 g, 2.76 mmol), EDC (0.53 g, 2.76 mmol), and DMAP (0.33 g, 0.28 mmol) were added under nitrogen at 0 °C and the reaction was stirred 0 °C for 6 h. The reaction mixture diluted with CH_2Cl_2 (150 mL) and water (100 mL) added, and the organic phase was washed with water (2×100 mL) and with brine (100 mL). The organic phase was dried, filtered, and concentrated under reduced pressure. The crude product was dissolved in hexanes/ethyl acetate (2:1) and passed through a silica gel column to produce **10b**, the title compound as a colorless liquid (0.90 mg, 50% yield). Rf = 0.22. 3:7 EtOAc/hexanes. of α and β anomers recovered: ^{1}H NMR (300 MHz, $CDCl_3$) δ_{ppm} 5.47 (t, J = 9.94, 1H), 5.32 (t, J = 5.65, 1H), 5.12–4.98 (m, 2H), 4.9 (d, J = 10.05, 1H), 4.05–4.3 (m, 5H), 3.89–3.63 (m, 2H), 3.54–3.50 (m, 1H), 2.41–2.29 (m, 2H), 2.11 (s, 3H), 2.08 (s, 3H), 2.04 (s, 3H), 2.03(s, 3H), 1.61 (m, 2H), 1.31 (s, 24H), 0.91 (t, J = 6.96, 3H).

1-*O*-Hexadecanoyl-2-*O*-*cis*-octadec-12-enoyl-3-*O*-(*α*-D-2,3,4,6-tetra-*O*-acetyl-glucopyranosyl)-sn-glycerol (10c) and 1-*O*-hexadecanoyl-2-*O*-*cis*-octadec-12-enoyl-3-*O*-(*β*-D-2,3,4,6-tetra-*O*-acetyl-glucopyranosyl)-sn-glycerol (10d): To a solution of compound **10b** (0.85 g, 1.29 mmol) in anhydrous CH_2Cl_2 (30 mL), *cis*-vaccenic acid (0.43 g, 1.52 mmol), EDC (0.30 g, 1.52 mmol), and DMAP (6 pinches) were added under nitrogen at 0 °C and the reaction was stirred for 16 h at room temperature. CH_2Cl_2 (50 mL) and water (50 mL) were added to the reaction mixture and the organic phase was washed with water (2×40 mL) and brine (40 mL). The organic phase was dried, filtered, and concentrated under reduced pressure. The crude product was dissolved in hexanes/ethyl acetate (2:1) and passed through a silica gel column to produce α-compound **10c**, the title compound as a colorless liquid (0.70 g, 58% yield). Rf = 0.33 (30% EtOAc, 70% Hexane). ^{1}H NMR (500 MHz, $CDCl_3$) δ_{ppm} 5.44 (t, J = 9.87, 1H), 5.34–5.25 (m, 2H), 5.20–5.11 (m, 1H), 5.09–5.06 (m, 1H), 5.05 (d, J = 9.80, 1H) 4.85 (dd, J = 3.79, 10.27, 1H), 4.32 (td, J = 4.27, 11.70, 1H), 4.24 (dt, J = 3.69, 12.37, 1H), 4.14–4.10 (m, 1H), 4.09–4.03 (m, 1H), 4.01 (t, J = 9.82, 1H), 3.81 (dd, J = 4.76, 11.17, 1H), 3.62–3.51 (m, 1H), 2.32–2.28 (m, 4H), 2.09–2.01(acetate singlets plus H2CCH=CHCH2, m, 16H), 1.62 (t, J = 6.87, 4H), 1.29 (s, 44H), 0.88 (td, J = 1.65, 6.83, 6H), and β-compound **10d** (0.48 g, 40% yield). Rf = 0.31 (30% EtOAc, 70% Hexane). ^{1}H NMR (500 MHz, $CDCl_3$) δ_{ppm} 5.32 (t, J = 4.73, 4.73 Hz, 2H), 5.24–5.12 (m, 2H), 5.11–5.02 (m, 1H), 5.01–4.92 (m, 1H), 4.51 (dd, J = 7.86, 4.03 Hz, 1H), 4.39–4.17 (m, 2H), 4.18–3.99 (m, 2H), 3.93 (dd, J = 10.95, 4.87 Hz, 1H), 3.75–3.55 (m, 2H), 2.39–2.16 (m, 4H), 2.10–1.89 (m, 16H), 1.68–1.50 (m, 4H), 1.36–1.18 (m, 44H), 0.86 (t, J = 6.10, 6.10 Hz, 6H).

(2*R*,4*aR*,6*R*,7*R*,8*S*,8*aR*)-2-Phenyl-7-(((2*R*,3*R*,4*S*,5*S*,6*R*)-3,4,5-tris(benzyloxy)-6-((benzyloxy)methyl)tetrahydro-2*H*-pyran-2-yl)oxy)hexahydropyrano[3,2-*d*][1,3]dioxine-6,8-diyl diacetate (15): Acceptor **13** (3.00 g, 8.52 mmol, prepared according to Ensley;[33] and standard trichloroacetimidate donor **14** (9.70 g, 14.2 mmol)[34] were dissolved in CH_2Cl_2 (500 mL) and (10 g) activated 5 Å MS was added and stirred at room temperature for 30 min, and then cooled to 0 °C. $BF_3{\cdot}OEt_2$ (1.1 mL, 8.52 mmol) was then added dropwise and stirred for 4 h at room temperature. The mixture passed through a pad of Celite and solvent concentrated under reduced pressure. The crude product was dissolved in hexanes/ethyl acetate (9:1) and passed through a silica gel column to produce **15**, title compound as a colorless liquid (3.80 g, 50% yield). Rf = 0.34. 3:7 EtOAc/hexanes. ^{1}H NMR (500 MHz, $CDCl_3$) δ_{ppm} 7.47–7.39 (m, 2H), 7.40–7.27 (m, 21H), 7.26–7.24 (m, 2H), 6.35 (d, J = 3.73 Hz, 1H), 5.55 (t, J = 9.77, 9.77 Hz, 1H), 5.46 (s, 1H), 4.90 (dd, J = 17.93, 7.44 Hz, 2H), 4.80 (d, J = 11.78 Hz, 1H), 4.73 (dd, J = 11.65, 2.51 Hz, 2H), 4.62 (d, J = 11.83 Hz, 1H), 4.52 (d, J = 11.36 Hz, 1H), 4.47 (d, J = 11.77 Hz, 1H), 4.40 (d, J = 11.69 Hz, 1H), 4.32–4.27 (m, 1H), 4.03–3.89 (m, 5H), 3.85 (dd, J = 10.13, 2.69 Hz, 1H), 3.68 (t, J = 10.32, 10.32 Hz, 1H), 3.59–3.51 (m, 2H), 3.50 (dd, J = 8.89, 5.55 Hz, 1H), 1.99 (s, 3H), 1.94 (s, 3H). ^{13}C NMR (125 MHz, $CDCl_3$) δ_{ppm} 170.0, 169.7, 138.9, 138.8, 138.7, 138.6, 138.0, 137.0, 129.7, 129.2, 128.5, 128.4, 128.4, 128.3, 128.1, 128.0, 127.9, 127.7, 127.5, 127.4, 127.2, 126.2, 103.8, 101.6, 99.9, 97.6, 89.3, 79.2, 78.8, 75.5, 75.2, 75.0, 74.8, 74.1, 73.6, 73.6, 73.4, 73.3, 73.2, 73.1, (1 peaks is covered under $CDCl_3$ peaks), 72.7, 70.2, 70.0, 69.9, 68.8, 68.7, 68.5, 64.7, 21.0, 20.8. **EI-MS *m/z*** calcd for $C_{51}H_{54}O_{13}$ 874.3612 $[M]^+$; $C_{51}H_{58}NO_{13}$ 892.3908 $[M+NH_4]^+$; Found: 892.3909.

(2*R*,4*aR*,7*R*,8*S*,8*aR*)-6-Hydroxy-2-phenyl-7-(((2*R*,3*R*,4*S*,5*S*,6*R*)-3,4,5-tris(benzyloxy)-6-((benzyloxy)methyl)tetrahydro-2*H*-pyran-2-yl)oxy)hexahydropyrano[3,2-*d*][1,3]dioxin-8-yl acetate (16): Compound **15** (8.00 g, 9.15 mmol) was dissolved in THF (550 mL) and prepared salt of ethyleneamine and acetic acid (18.0 g) was added, which was formed by mixing acetic acid (36 mL) with ethylene diamine (29 mL) at room temperature to 0 °C for 15 minutes. The reaction mixture was stirred at room temperature for 24 h. The mixture was concentrated, then CH_2Cl_2 (300 mL) was added and the organic phase was washed with water (2×200 mL) and with brine (200 mL). The organic phase was dried, filtered, and concentrated under reduced pressure. The crude product was dissolved in hexanes/ethyl acetate (9:1) and passed through a silica gel column to produce **16**, the title compound as a white solid, mixtures of α and β anomers (ratio: 1/1 determined by ^{1}H NMR) (3.00 g, 40% yield). Rf = 0.31. 1:9 EtOAc/hexanes. ^{1}H NMR (500 MHz, $CDCl_3$) δ_{ppm} 7.44–7.20 (m, 25H), 5.45 (d, J = 4.52 Hz, 2H), 5.31 (t, J = 9.32, 9.32 Hz, 1H), 4.97–4.82 (m, 3H), 4.78–4.65 (m, 4H), 4.53 (dd, J = 11.31, 6.53 Hz, 1H), 4.44 (dd, J = 24.09, 11.80 Hz, 2H), 4.38–4.30 (m, 1H), 4.08–3.87 (m, 4H), 3.82–3.71 (m, 1H), 3.63–3.47 (m, 3H), 3.46 (dd, J = 6.32, 5.10 Hz, 1H), 3.43–3.37 (m, 1H), 1.97 (s, 3H). ^{13}C NMR (125 MHz, $CDCl_3$) δ_{ppm} 170.1, 138.7, 138.5, 138.4, 138.3, 137.9, 137.8, 137.6, 137.3, 137.2, 137.1, 128.8, 128.6, 128.4, 128.3, 128.1, 127.8, 127.6, 127.6, 126.3, 126.3, 101.5, 101.5, 97.5, 97.3, 91.3, 84.4, 79.6, 79.3, 79.1, 78.9, 75.2, 75.1, 74.5, 74.4, 73.7, 73.6, 73.0, 72.6, 71.9, 70.7, 70.1, 69.0, 68.8, 68.0, 67.0, 63.0, 60.5, 14.3. **EI-MS *m/z*** calcd for $C_{49}H_{52}O_{12}$ 832.3401 $[M]^+$; $C_{49}H_{56}NO_{12}$ $[M+NH_4]^+$ 850.3803. Found: 850.3806.

(2*R*,4*aR*,6*S*,7*R*,8*S*,8*aR*)-6-(((*S*)-2,2-Dimethyl-1,3-dioxolan-4-yl)methoxy)-2-phenyl-7-(((2*R*,3*R*,4*S*,5*S*,6*R*)-3,4,5-tris(benzyloxy)-6-((benzyloxy)methyl)tetrahydro-2*H*-pyran-2-yl)oxy)hexahydropyrano[3,2-*d*][1,3]dioxin-8-yl acetate (17): Compound **16** (50.0 mg, 0.06 mmol) and diphenylsulfoxide (36.0 mg, 0.17 mmol) were stirred over (130 mg) of activated 4 Å MS for 45 min in CH_2Cl_2 (4 mL), then the mixture was cooled to −78 °C, and triflic anhydride (14 μL, 0.08 mmol) and 2-chloropyridine (30 μL, 0.32 mmol) were added and warmed to −40 °C and stirred for 45 min, then compound **8** (25.0 mg, 0.19 mmol) in CH_2Cl_2 (1 mL) was added and allowed to stir for 16 h. The reaction mixture was quenched with Et_3N (0.5 mL). The mixture passed through a pad of Celite and washed with CH_2Cl_2 (50 mL). The organic phase was washed with water (2×30 mL), saturated aqueous $NaHCO_3$ (30 mL) and brine (30 mL). The organic phase was dried, filtered, and concentrated under reduced pressure. The crude product was dissolved in hexanes/ethyl acetate (10:1) and passed through a silica gel column to produce **17**, the title compound as a colorless liquid compound (25.0 mg, 46% yield). Rf = 0.36. 1:9 EtOAc/hexanes. ^{1}H NMR (500 MHz, $CDCl_3$) δ_{ppm} 7.71–7.60 (m, 1H), 7.48–7.42 (m, 3H), 7.37–7.28 (m, 19H), 7.41–7.38 (m, 2H), 5.52 (t, *J* = 9.72, 9.72 Hz, 1H), 5.45 (s, 1H), 5.00 (d, *J* = 3.58 Hz, 1H), 4.94 (dd, *J* = 7.38, 3.88 Hz, 2H), 4.79 (dd, *J* = 21.55, 11.34 Hz, 3H), 4.68 (d, *J* = 11.53 Hz,

1H), 4.56 (d, J = 11.32 Hz, 1H), 4.45 (dd, J = 30.60, 11.78 Hz, 2H), 4.27 (dd, J = 10.27, 4.93 Hz, 1H), 4.17–4.11 (m, 1H), 4.06–3.97 (m, 3H), 3.96–3.88 (m, 3H), 3.79–3.63 (m, 3H), 3.61–3.55 (m, 2H), 3.52–3.45 (m, 2H), 3.41 (dd, J = 10.63, 5.01 Hz, 1H), 1.96 (s, 3H), 1.41 (s, 3H), 1.31 (s, 3H)) ^{13}C NMR (125 MHz, $CDCl_3$) δ_{ppm} 169.8, 138.7, 138.7, 138.6, 138.0, 137.1, 131.1, 129.4, 129.1, 129.0, 128.4, 128.3, 128.2, 128.0, 127.8, 127.7, 127.6, 127.5, 126.2, 124.8, 109.4, 101.5, 98.7, 97.8, 79.7, 78.8, 77.1, (12 peaks are covered under $CDCl_3$ peaks), 74.9, 74.9, 74.4, 73.5, 73.4, 72.8, 70.1, 70.0, 69.0, 68.9, 68.3, 66.7, 62.6, 26.7, 25.6, 21.0. **EI-MS *m/z*** calcd for $C_{55}H_{62}O_{14}$ 946.4104 $[M]^+$; $C_{55}H_{62}O_{14}Na$ $[M+Na]^+$ 969.4037. Found: 969.4030.

(2*R*,4*aR*,6*S*,7*R*,8*S*,8*aS*)-6-(((*S*)-2,2-Dimethyl-1,3-dioxolan-4-yl)methoxy)-2-phenyl-7-(((2*R*,3*R*,4*S*,5*S*,6*R*)-3,4,5-tris(benzyloxy)-6-((benzyloxy)methyl)tetrahydro-2*H*-pyran-2-yl)oxy)hexahydropyrano[3,2-*d*][1,3]dioxin-8-ol (17 a): To a solution of compound **17** (90.0 mg, 0.09 mmol) in methanol (50 mL), solution of sodium methoxide was added until a pH of 12 was reached, then stirred for 16 h. Dowex 50WX8 was added to neutralize solution. Mixture filtered and concentrated under reduced pressure. The crude product was dissolved in hexanes/ethyl acetate (7:3) and passed through a silica gel column to produce **17 a**, title compound as a colorless liquid (60.0 mg, 70% yield). Rf = 0.36. 2:8 EtOAc/hexanes. ^{1}H NMR (500 MHz, $CDCl_3$) δ_{ppm} 7.56–7.49 (m, 2H), 7.43–7.34 (m, 19H), 7.34–7.25 (m, 4H), 5.53 (s, 1H), 5.05 (d, J = 3.75 Hz, 1H), 4.95 (dd, J = 7.59, 3.90 Hz, 2H), 4.84 (d, J = 11.55 Hz, 2H), 4.77 (d, J = 11.88 Hz, 1H), 4.69 (d, J = 11.74 Hz, 1H), 4.58 (d, J = 11.51 Hz, 1H), 4.51 (d, J = 11.75 Hz, 1H), 4.41 (d, J = 11.75 Hz, 1H), 4.29 (dd, J = 10.22, 4.83 Hz, 1H), 4.26–4.19 (m, 2H), 4.13–4.07 (m, 2H), 4.02–3.87 (m, 4H), 3.83 (dd, J = 8.28, 6.29 Hz, 1H), 3.77–3.65 (m, 3H), 3.60–3.49 (m, 3H), 3.49–3.39 (m, 2H), 1.43 (s, 3H), 1.35 (s, 3H) ^{13}C NMR (125 MHz, $CDCl_3$) δ_{ppm} 138.6, 138.5, 138.4, 137.8, 137.2, 129.1, 128.4, 128.4, 128.3, 128.3, 128.2, 127.9, 127.8, 127.7, 127.7, 127.6, 127.5, 126.4, 109.4, 102.0, 98.3, 98.1, 81.1, 81.1, 78.8, 77.6, 76.3, 74.8, 74.7, 74.5, 73.5, 73.4, 73.0 (11 peaks are covered under $CDCl_3$ peaks), 69.3, 69.2, 69.0, 68.9, 66.6, 62.5, 62.5, 26.7, 25.5. **EI-MS *m/z*** calcd for $C_{53}H_{60}O_{13}$ 904.4034 $[M]^+$; $C_{53}H_{60}O_{13}Na$ $[M+Na]^+$ 927.3932. Found: 927.3926.

(2*R*,3*R*,4*S*,5*R*,6*R*)-2-(((2*S*,3*R*,4*S*,5*S*,6*R*)-2-(((*S*)-2,2-Dimethyl-1,3-dioxolan-4-yl)methoxy)-4,5-dihydroxy-6-(hydroxymethyl)tetrahydro-2*H*-pyran-3-yl)oxy)-6-(hydroxymethyl)tetrahydro-2*H*-pyran-3,4,5-triol (18): To a solution of acetyl deprotected of **17 a** (60.0 mg, 0.06 mmol) in MeOH (3 mL), Pd/C (400 mg, 1.86 mmol) and ammonium formate (230 mg, 3.65 mmol) were added and refluxed at 70 °C for 7 h. After cooling to room temperature, the reaction mixture was then passed through a pad of Celite and washed with MeOH (20 mL). The solvent was concentrated under reduced pressure and then co-evaporated with toluene. The crude product was dissolved in ethyl acetate/methanol (9.5:0.5) and passed through a silica gel column to produce **18**, title compound as a colorless liquid (23.0 mg, 73% yield). Rf = 0.29. 95:5 EtOAc/MeOH. ^{1}H NMR (500 MHz, MeOD) δ_{ppm} 5.12 (d, J = 3.55 Hz, 1H), 5.06 (d, J = 3.73 Hz, 1H), 4.69–4.51 (m, 2H), 4.44–4.30 (m, 1H), 4.19–4.02 (m, 3H), 3.92 (dd, J = 3.12, 1.08 Hz, 1H), 3.87–3.66 (m, 12H), 3.66–3.55 (m, 4H), 3.38 (d, J = 9.80 Hz, 1H), 1.43 (s, 3H), 1.37 (s, 3H) ^{13}C NMR (125 MHz, MeOD) δ_{ppm} 109.3, 96.8, 96.3, 76.2, 74.8, 73.1, 72.3, 72.0, 71.1, 70.2, 70.1, 69.8, 68.9, 68.5, 66.2, 61.4, 61.3, 25.7, 24.3. **EI-MS *m/z*** calcd for $C_{18}H_{32}O_{13}$ 456.1843; $C_{18}H_{32}O_{13}$ $[M+Na]^+$ 479.1741. Found: 479.1732.

(2*R*,3*R*,4*S*,5*S*,6*R*)-2-(((2*S*,3*R*,4*S*,5*R*,6*R*)-2-(((*S*)-2,2-Dimethyl-1,3-dioxolan-4-yl)methoxy)-4,5-bis(2-methoxyacetoxy)-6-((2-methoxyacetoxy)methyl)tetrahydro-2*H*-pyran-3-yl)oxy)-6-((2-methoxyacetoxy)methyl)tetrahydro-2*H*-pyran-3,4,5-triyl tris(2-methoxyacetate) (18 a): Compound **18** (40.0 mg, 0.09 mmol) was dissolved in pyridine (2 mL), and cooled to 0 °C, then methoxyacetyl chloride (3 mL, 1.10 mmol) was added dropwise and stirred for 16 h. The reaction mixture diluted with EtOAc (50 mL) and the organic phase was washed with 10% HCl aq. (30 mL), water (30 mL) and brine (30 mL). The organic phase was dried, filtered, and concentrated under reduced pressure. The crude product was dissolved in hexanes/ethyl acetate (2:8) and passed through a silica gel column to produce **18 a**, title compound as a yellow liquid (60.0 mg, 72% yield). Rf = 0.3. 2:8 EtOAc/hexanes. ^{1}H NMR (500 MHz, $CDCl_3$) δ_{ppm} 5.55–5.48 (m, 2H), 5.38–5.31 (m, 2H), 5.13 (dd, J = 10.77, 3.50 Hz, 1H), 5.10–5.04 (m, 2H), 4.40–4.34 (m, 2H), 4.33–4.26 (m, 2H), 4.25–3.93 (m, 17H), 3.86 (d, J = 16.51 Hz, 1H), 3.82 (dd, J = 9.95, 3.54 Hz, 1H), 3.73 (ddd, J = 15.34, 9.62, 5.30 Hz, 2H), 3.59 (dd, J = 10.96, 5.67 Hz, 1H), 3.46–3.39 (m, 21H), 1.43 (s, 3H), 1.36 (s, 3H) ^{13}C NMR (125 MHz, $CDCl_3$) δ_{ppm} 170.0, 169.8, 169.8, 169.7, 169.6, 169.4, 169.3, 109.8, 95.8, 94.8, 74.5, 74.5, 71.8, 69.7, 69.5, 69.3, 69.0, 68.6, 68.3, 68.2, 68.1, 67.5, 67.3, 67.1, 66.2, 61.9, 61.0, 61.0, 59.5, 59.4, 38.8, 30.4, 29.0. 26.7, 25.4, 23.8, 23.0, 14.1, 11.0. **EI-MS *m/z*** calcd for $C_{39}H_{60}O_{27}$ $[M]^+$ 960.3322; $C_{39}H_{60}O_{27}Na$ $[M+Na]^+$ 983.3220. Found: 983.3232.

(2*R*,3*R*,4*S*,5*S*,6*R*)-2-(((2*S*,3*R*,4*S*,5*R*,6*R*)-2-((*R*)-2,3-Dihydroxypropoxy)-4,5-bis(2-methoxyacetoxy)-6-((2-methoxyacetoxy)methyl)tetrahydro-2*H*-pyran-3-yl)oxy)-6-((2-methoxyacetoxy)methyl)tetrahydro-2*H*-pyran-3,4,5-triyl tris(2-methoxyacetate) (20): Compound **18 a** (17.0 mg, 0.02 mmol) was dissolved in acetonitrile (2 mL) and $Zn(NO_3)_2.6H_2O$ (32.0 mg, 0.11 mmol) was added. The mixture was stirred for 6 h at 50 °C, and the solvent was then evaporated under reduced pressure, then CH_2Cl_2 (30 mL) was added and the organic phase was washed with water (20 mL) and brine (20 mL). The organic phase was dried, filtered, and concentrated under reduced pressure. The crude product was dissolved in methanol/ethyl acetate (1:9) and passed through a silica gel column to produce **20**, title compound as a colorless liquid (15.0 mg, 96% yield). Rf = 0.38. 9:1 EtOAc/MeOH. ^{1}H NMR (500 MHz, MeOD) δ_{ppm} 5.59 (dd, J = 3.27, 1.21 Hz, 1H), 5.55 (t, J = 9.69, 9.69 Hz, 1H), 5.44 (d, J = 3.60 Hz, 1H), 5.38 (dd, J = 10.80, 3.42 Hz, 1H), 5.24 (dd, J = 10.76, 3.57 Hz, 1H), 5.20 (d, J = 3.52 Hz, 1H), 5.11 (dd, J = 10.20, 9.40 Hz, 1H), 4.47–4.39 (m, 2H), 4.36 (dd, J = 11.11, 6.25 Hz, 1H), 4.27–4.17 (m, 6H), 4.16–3.98 (m, 12H), 3.92 (d, J = 17.02 Hz, 1H), 3.89–3.81 (m, 2H), 3.67–3.59 (m, 2H), 3.57 (dd, J = 10.03, 6.05 Hz, 1H), 3.50–3.38 (m, 22H) ^{13}C NMR (125 MHz, MeOD) δ_{ppm} 171.9, 171.9, 171.8, 171.7, 171.5, 171.2, 171.1, 97.3, 96.0, 75.2, 73.2, 72.1, 71.0, 70.7, 70.6, 70.4, 70.4, 70.2, 70.2, 70.2, 70.1, 69.8, 69.3, 69.2, 68.6, 68.5, 64.2, 63.2, 62.8, 61.6, 59.8, 59.7, 59.7, 59.6, 59.6, 59.5. **EI-MS *m/z*** calcd for $C_{36}H_{56}O_{27}$ $[M]^+$ 920.3009; $C_{36}H_{57}O_{27}$ $[M+H]^+$ 921.3087. Found: 921.3085.

(2*R*,3*R*,4*S*,5*S*,6*R*)-2-(((2*S*,3*R*,4*S*,5*R*,6*R*)-2-((*S*)-2-Hydroxy-3-(palmitoyloxy)propoxy)-4,5-bis(2-methoxyacetoxy)-6-((2-methoxyacetoxy)methyl)tetrahydro-2*H*-pyran-3-yl)oxy)-6-((2-methoxyacetoxy)methyl)tetrahydro-2*H*-pyran-3,4,5-triyl tris(2-methoxyacetate) (20 a): Compound **20** (12.0 mg, 0.01 mmol), was dissolved in anhydrous CH_2Cl_2 (2 mL) under nitrogen and palmitic acid (4.00 mg), 0.01 mmol), EDC (2.50 mg, 0.01 mmol), and DMAP (2 pinches) were added under nitrogen at 0 °C and the reaction was stirred on ice for 6 h. then CH_2Cl_2 (20 mL) was added and the organic phase was washed with water (10 mL) and brine (10 mL). The organic phase was dried, filtered, and concentrated under reduced pressure. The crude product was dissolved in ethyl acetate and passed through a silica gel column to produce **20 a**, title compound as a colorless liquid (8.00 mg, 53% yield). Rf = 0.55 EtOAc. ^{1}H NMR (500 MHz, $CDCl_3$) δ_{ppm} 5.62–5.45 (m, 2H), 5.41–5.29 (m, 2H) 5.18–5.02 (m, 3H), 4.43–4.34 (m, 2H), 4.34–4.25 (m, 1H), 4.21–3.95 (m, 19H), 3.90 (s, 1H), 3.88–3.82 (m, 1H), 3.77 (dd, J = 11.03, 3.09 Hz, 1H), 3.53 (dd, J = 10.97, 7.30 Hz, 1H), 3.49–3.33 (m, 21H), 3.06 (d, J = 4.27 Hz, 1H), 2.36–2.32 (m, 2H), 1.66–1.60 (m, 2H), 1.37–1.17 (m, 24H), 0.89 (t, J = 6.96, 6.96 Hz, 3H) ^{13}C NMR (125 MHz, $CDCl_3$) δ_{ppm} 174.0, 170.2, 170.1, 170.1, 170.0, 169.9, 169.8, 169.6,

169.5, 168.9, 96.5, 94.7, 74.5, 74.3, 71.8, 70.4, 69.8, 69.7, 69.5, 69.3, 68.8, 68.2, 67.7, 67.5, 67.4, 67.2, 65.2, 62.1, 61.2, 59.7, 59.6, 59.6, 34.2, 32.1, 29.9, 29.9, 29.8, 29.8, 29.7, 29.5, 29.5, 29.4, 29.4, 29.3, 29.3, 29.1, 27.4, 27.3, 25.0, 22.9, 14.3, 14.2. **EI-MS *m/z*** calcd for $C_{52}H_{86}O_{28}$ 1158.5306 $[M]^+$; $C_{52}H_{87}O_{28}$ 1159.5384 $[M+H]^+$; $C_{52}H_{87}O_{28}$ 1159.5339 $[M-H+D]^+$. Found: 1159.5343.

(2*R*,3*R*,4*S*,5*S*,6*R*)-2-(((2*S*,3*R*,4*S*,5*R*,6*R*)-4,5-Bis(2-methoxyacetoxy)-6-((2-methoxyacetoxy)methyl)-2-((*S*)-2-((*Z*)-octadec-6-enoyloxy)-3-(palmitoyloxy)propoxy)tetrahydro-2*H*-pyran-3-yl)oxy)-6-((2-methoxyacetoxy)methyl)tetrahydro-2*H*-pyran-3,4,5-triyl tris(2-methoxyacetate) (21): Compound **20a** (11.0 mg, 0.01 mmol) was dissolved in anhydrous CH_2Cl_2 (2 mL) under nitrogen and *cis*-vaccenic acid (4.00 mg, 0.01 mmol), EDC (3.00 mg, 0.01 mmol), and DMAP (2 pinches) were added under nitrogen at 0 °C and the reaction was stirred on ice for 16 h. then CH_2Cl_2 (20 mL) was added and the organic phase was washed with water (10 mL) and brine (10 mL). The organic phase was dried, filtered, and concentrated under reduced pressure. The crude product was dissolved in hexanes/ethyl acetate (1:3) and passed through a silica gel column to produce **21**, title compound as a colorless liquid (7.00 mg, 50% yield). Rf = 0.4. 2.5:7.5 EtOAc/hexanes. ^{1}H NMR (500 MHz, $CDCl_3$) δ_{ppm} 5.57–5.50 (m, 1H), 5.47 (t, J = 9.56, 9.56 Hz, 1H), 5.39 (dd, J = 10.70, 3.27 Hz, 1H), 5.36–5.33 (m, 2H), 5.27 (d, J = 3.51 Hz, 1H), 5.25–5.18 (m, 1H), 5.15 (dd, J = 10.76, 3.54 Hz, 1H), 5.10–5.02 (m, 1H), 5.00 (d, J = 3.52 Hz, 1H), 4.46–4.33 (m, 3H), 4.29 (dd, J = 11.08, 7.13 Hz, 1H), 4.23 (dd, J = 12.01, 6.49 Hz, 1H), 4.19–3.94 (m, 16H), 3.90–3.77 (m, 3H), 3.71 (dd, J = 10.93, 4.75 Hz, 1H), 3.52–3.31 (m, 21H), 2.40–2.25 (m, 4H), 2.06–1.96 (m, 4H), 1.70–1.61 (m, 4H), 1.39–1.09 (m, 44H), 0.92–0.83 (m, 6H) ^{13}C NMR (125 MHz, $CDCl_3$) δ_{ppm} 173.5, 173.1, 172.0, 170.1, 170.0, 170.0, 170.0, 169.9, 169.8, 169.7, 169.5, 169.4, 169.4, 169.3, 169.3, 164.56, 130.1, 130.0, 96.8, 96.2, 92.2, 91.9, 75.8, 72.0, 69.8, 69.1, 69.6, 69.5, 69.5, 69.4, 68.6, 68.6, 68.3, 67.7, 67.6, 67.6, 67.5, 67.3, 62.4, 61.9, 61.8, 61.1, 59.6, 59.6, 59.5, 34.4, 34.2, 32.1, 31.9, 30.0, 29.9, 29.9, 29.8, 29.7, 29.7, 29.7, 29.5, 29.4, 29.4, 29.3, 29.3, 29.2, 29.1, 27.4, 25.1, 25.0, 22.8, 22.8, 14.3, 14.2. **EI-MS *m/z*** calcd for $C_{70}H_{118}O_{29}$ 1422.7759 $[M]^+$; $C_{70}H_{119}O_{29}$ 1423.7837 $[M+H]^+$. Found: 1423.7827.

All synthetic experimental details, including spectra for all new compounds, is provided in the Supporting Information. All biological data, including details about the studies conducted and the animal models used, is provided in the Supporting Information.. Computational protocols and additional figures with alternative views are also available in the Supporting Information.

Author Contributions

Conceptualization, JFT; Funding acquisition JFT, MR; Investigation, SIS, EI, GY, MK, SM, SMT, RA, JT; Methodology, SIS, SMT, MR, JFT; Visualization, SMT, MK, MR; Project administration, JFT, MR; Supervision, JFT, MR; Writing original draft, SIS, SMT, JFT, MR; Writing – review and editing, All authors.

Acknowledgements

The authors gratefully acknowledge financial support for the project from the Windsor Cancer Centre Foundation (2019-003), the Natural Sciences and Engineering Research Council of Canada (J. F. T.: grant #2018-06338), the Canadian Tricouncil (NFRFE-2018-00075). S. M. T. and J. F. T. wish to recognize that this work was made possible by the facilities of the Shared Hierarchical Academic Research Computing Network (SHARCNET: www.sharcnet.ca) and Compute/Calcul Canada. The authors would like to thank Chelsea Ymana, and Science Meets Art UWindsor, for executing the TOC graphic. J. F. T. would like to thank S. Mansour Haeryfar of the University of Western Ontario for initiating the idea behind this study.

Conflict of Interest

The authors declare no conflict of interest.

Data Availability Statement

The data that support the findings of this study are available in the supplementary material of this article.

Keywords: carbohydrate synthesis · glycolipids · invariant natural killer T cells · KRN7000 · *S. pneumoniae*

[1] L. Tao, T. A. Reese, *Tr. Immunol.* **2017**, *38*, 181–193.
[2] D. I. Godfrey, A. P. Uldrich, J. McCluskey, J. Rossjohn, D. B. Moody, *Nat. Immunol.* **2015**, *16*, 1114–1123.
[3] M. Salio, J. D. Silk, E. Yvonne Jones, V. Cerundolo, *Ann. Rev. Immunol.* **2014**, *32*, 323–366.
[4] a) P. J. Brennan, M. Brigl, M. B. Brenner, *Nat. Rev. Immunol.* **2013**, *13*, 101–117; b) T. Tashiro, K. Mori, in *Glycosphingolipid Ligands for Invariant Natural Killer T cells as Immunostimulants, Vol. 42* Elsevier, **2014**, pp. 1–31.
[5] T. Natori, M. Morita, K. Akimoto, Y. Koezuka, *Tetrahedron* **1994**, *50*, 2771–2784.
[6] A. M. Birkholz, M. Kronenberg, *Biomed. J.* **2015**, *38*, 470–483.
[7] A. Banchet-Cadeddu, E. Henon, M. Dauchez, J.-H. Renault, F. Monneaux, A. Haudrechy, *Org. Biomol. Chem.* **2011**, *9*, 3080–3104.
[8] a) J. Novak, A. Lehuen, *Cytokine* **2011**, *53*, 263–270; b) C. M. Crosby, M. Kronenberg, *Immunogenetics* **2016**, *68*, 639–648; c) E. E. Nieuwenhuis, T. Matsumoto, M. Exley, R. A. Schleipman, J. Glickman, D. T. Bailey, N. Corazza, S. P. Colgan, A. B. Onderdonk, R. S. Blumberg, *Nat. Med.* **2002**, *8*, 588–593.
[9] Y. Kinjo, P. Illarionov, J. L. Vela, B. Pei, E. Girardi, X. Li, Y. Li, M. Imamura, Y. Kaneko, A. Okawara, Y. Miyazaki, A. Gomez-Velasco, P. Rogers, S. Dahesh, S. Uchiyama, A. Khurana, K. Kawahara, H. Yesilkaya, P. W. Andrew, C.-H. Wong, K. Kawakami, V. Nizet, G. S. Besra, M. Tsuji, D. M. Zajonc, M. Kronenberg, *Nat. Immunol.* **2011**, *12*, 966–974.
[10] R. Cherazard, M. Epstein, T.-L. Doan, T. Salim, S. Bharti, M. A. Smith, *Am. J. Ther.* **2017**, *24*, e361–e369.
[11] B. M. Gray, D. M. Musher, in *The History of Pneumococcal Disease*, American Society of Microbiology, **2008**.
[12] a) C. Ratledge, in *Microbial Production of Vitamin F and Other Polyunsaturated Fatty Acids*, Wiley-VCH, Weinheim, **2016**, pp. 287–320; b) A. Shibahara, K. Yamamoto, M. Takeoka, A. Kinoshita, G. Kajimoto, T. Nakayama, M. Noda, *FEBS Lett.* **1990**, *268*, 306–306; c) A. Shibahara, K. Yamamoto, M. Takeoka, A. Kinoshita, G. Kajimoto, T. Nakayama, M. Noda, *FEBS Lett.* **1990**, *264*, 228–230.
[13] C. J. Field, H. H. Blewett, S. Proctor, D. Vine, *Appl. Physiol. Nutr. Metab.* **2009**, *34*, 979–991.
[14] M. Shimamura, H. Hidaka, *Curr. Med. Chem.* **2012**, *19*, 4869–4874.
[15] M. B. Richardson, D. G. M. Smith, S. J. Williams, *Chem. Commun.* **2017**, *53*, 1100–1103.
[16] a) S. Burugupalli, C. F. Almeida, D. G. M. Smith, S. Shah, O. Patel, J. Rossjohn, A. P. Uldrich, D. I. Godfrey, S. J. Williams, *Chem. Sci.* **2020**, *11*, 2161–2168; b) C. F. Almeida, S. Sundararaj, J. Le Nours, T. Praveena, B. Cao, S. Burugupalli, D. G. M. Smith, O. Patel, M. Brigl, D. G. Pellicci, S. J. Williams, A. P. Uldrich, D. I. Godfrey, J. Rossjohn, *Nat. Commun.* **2019**, *10*, 5242.
[17] T. Imai, T. Matsumura, S. Mayer-Lambertz, C. A. Wells, E. Ishikawa, S. K. Butcher, T. C. Barnett, M. J. Walker, A. Imamura, H. Ishida, T. Ikebe, T.

Miyamoto, M. Ato, S. Ohga, B. Lepenies, N. M. v. Sorge, S. Yamasaki, *Proc. Natl. Acad. Sci. USA* **2018**, *115*, E10662–E10671.
[18] A. J. Webb, M. Karatsa-Dodgson, A. Gründling, *Mol. Microbiol.* **2009**, *74*, 299–314.
[19] I. P. Dragalin, P. K. Kintia, *Phytochemistry* **1975**, *14*, 1817–1820.
[20] a) C. A. A. van Boeckel, J. H. van Boom, *Tetrahedron* **1985**, *41*, 4567–4575; b) K. Takato, M. Kurita, N. Yagami, H.-N. Tanaka, H. Ando, A. Imamura, H. Ishida, *Carbohydr. Res.* **2019**, *483*, 107748.
[21] a) V. Pozsgay, J. Kubler-Kielb, B. Coxon, A. Marques, J. B. Robbins, R. Schneerson, *Carbohydr. Res.* **2011**, *346*, 1551–1563; b) B. Ghosh, Y. H. Lai, Y. Y. Shih, T. K. Pradhan, C. H. Lin, K. K. T. Mong, *Chem. Asian J.* **2013**, *8*, 3191–3199; c) B. Cao, X. Chen, Y. Yamaryo-Botte, M. B. Richardson, K. L. Martin, G. N. Khairallah, T. W. Rupasinghe, R. M. O'Flaherty, R. A. O'Hair, J. E. Ralton, P. K. Crellin, R. L. Coppel, M. J. McConville, S. J. Williams, *J. Org. Chem.* **2013**, *78*, 2175–2190; d) S. D. Stamatov, J. Stawinski, *Org. Biomol. Chem.* **2010**, *8*, 463–477.
[22] J. Ohlsson, G. Magnusson, *Carbohydr. Res.* **2000**, *329*, 49–55.
[23] R. Katoch, G. K. Trivedi, R. S. Phadke, *Bioorg. Med. Chem.* **1999**, *7*, 2753–2758.
[24] The reaction was attempted using 4 different batches of starting material, by 5 different chemists, using 3 different fresh bottles of sodium periodate. Starting material proceeded directly to a complex mixture in all cases, and only trace amounts of the desired material were able to be isolated regardless of changes in temperature, solvent mixture, and additives. Lead(IV) acetate proceeds smoothly.
[25] F. Sugawara, H. Nakayama, G. A. Strobel, T. Ogawa, *Agric. Biol. Chem.* **1986**, *50*, 2251–2259.
[26] a) B. Ghosh, Y.-H. Lai, Y.-Y. Shih, T. K. Pradhan, C.-H. Lin, K.-K. T. Mong, *Chem. Asian J.* **2013**, *8*, 3191–3199; b) C.-T. Ren, Y.-H. Tsai, Y.-L. Yang, S.-H. Wu, *J. Org. Chem.* **2007**, *72*, 5427–5430.
[27] T. Sugiyama, H. Sugawara, M. Watanabe, K. Yamashita, *Agric. Biol. Chem.* **1984**, *48*, 1841–1844.
[28] S. Vijayasaradhi, J. Singh, I. S. Aidhen, *Synlett* **2000**, *2000*, 110–112.
[29] P. E. Duffy, S. M. Quinn, H. M. Roche, P. Evans, *Tetrahedron* **2006**, *62*, 4838–4843.
[30] Estimated by ^{1}H NMR analysis.
[31] E. Manzo, M. L. Ciavatta, D. Pagano, A. Fontana, *Tetrahedron Lett.* **2012**, *53*, 879–881.
[32] T. Jefferson, in *The Papers of Thomas Jefferson, Retirement Series Vol 5* (Ed. W. Duane), Princeton Press, Princeton, **1812**, pp. 293–294.
[33] H. Yu, H. E. Ensley, *Tetrahedron Lett.* **2003**, *44*, 9363–9366.
[34] D. J. Cox, M. D. Smith, A. J. Fairbanks, *Org. Lett.* **2010**, *12*, 1452–1455.
[35] A. V. Demchenko in *Handbook of Chemical Glycosylation*, Wiley-VCH, Weinheim, **2008**, p. 501.
[36] Y. Liu, S. Deng, L. Bai, S. Freigang, J. Mattner, L. Teyton, A. Bendelac, P. B. Savage, *Bioorg. Med. Chem. Lett.* **2008**, *18*, 3052–3055.
[37] B. A. Garcia, J. L. Poole, D. Y. Gin, *J. Am. Chem. Soc.* **1997**, *119*, 7597–7598.
[38] a) C. Reese, J. Stewart, *Tetrahedron Lett.* **1968**, *9*, 4273–4276; b) T. Hanamoto, Y. Sugimoto, Y. Yokoyama, J. Inanaga, *J. Org. Chem.* **1996**, *61*, 4491–4492; c) R. Rosseto, N. Bibak, R. DeOcampo, T. Shah, A. Gabrielian, J. Hajdu, *J. Org. Chem.* **2007**, *72*, 1691–1698.
[39] S. J. Williams, *Carbohydr. Res.* **2019**, *486*, 107848.
[40] a) J. L. Hayworth, D. M. Mazzuca, S. M. Vareki, I. Welch, J. K. McCormick, S. M. M. Haeryfar, *Immunol. Cell Biol.* **2012**, *90*, 699–709; b) P. A. Szabo, R. V. Anantha, C. R. Shaler, J. K. McCormick, S. M. M. Haeryfar, *Front. Immunol.* **2015**, *6*, 401–401; c) J. F. Trant, N. Jain, D. Mazzuca, J. McIntosh, B. Fan, S. M. M. Haeryfar, S. Lecommandoux, E. R. Gillies, *Nanoscale* **2016**, *8*, 17694–17704.
[41] a) J. Mattner, K. L. DeBord, N. Ismail, R. D. Goff, C. Cantu, D. Zhou, P. Saint-Mezard, V. Wang, Y. Gao, N. Yin, K. Hoebe, O. Schneewind, D. Walker, B. Beutler, L. Teyton, P. B. Savage, A. Bendelac, *Nature* **2005**, *434*, 525–529; b) E. Tupin, Y. Kinjo, M. Kronenberg, *Nat. Rev. Microbiol.* **2007**, *5*, 405.
[42] S. I. Sadraei, M. Reynolds, J. F. Trant, *Adv. Carbohydr. Chem. Biochem.* **2017**, *74*, 137–237.
[43] B. A. Wolucka, M. R. McNeil, L. Kalbe, C. Cocito, P. J. Brennan, *Biochim. Biophys. Acta Lipids Lipid Metab.* **1993**, *1170*, 131–136.
[44] A. P. Uldrich, O. Patel, G. Cameron, D. G. Pellicci, E. B. Day, L. C. Sullivan, K. Kyparissoudis, L. Kjer-Nielsen, J. P. Vivian, B. Cao, A. G. Brooks, S. J. Williams, P. Illarionov, G. S. Besra, S. J. Turner, S. A. Porcelli, J. McCluskey, M. J. Smyth, J. Rossjohn, D. I. Godfrey, *Nat. Immunol.* **2011**, *12*, 616–623.
[45] D. Szamosvári, M. Bae, S. Bang, B. K. Tusi, C. D. Cassilly, S.-M. Park, D. B. Graham, R. J. Xavier, J. Clardy, *J. Am. Chem. Soc.* **2022**, *144*, 2474–2478.
[46] M. Koch, V. S. Stronge, D. Shepherd, S. D. Gadola, B. Mathew, G. Ritter, A. R. Fersht, G. S. Besra, R. R. Schmidt, E. Y. Jones, V. Cerundolo, *Nat. Immunol.* **2005**, *6*, 819–826.
[47] E. Hénon, M. Dauchez, A. Haudrechy, A. Banchet, *Tetrahedron* **2008**, *64*, 9480–9489.
[48] N. A. Borg, K. S. Wun, L. Kjer-Nielsen, M. C. J. Wilce, D. G. Pellicci, R. Koh, G. S. Besra, M. Bharadwaj, D. I. Godfrey, J. McCluskey, J. Rossjohn, *Nature* **2007**, *448*, 44–49.
[49] M. Wernerova, T. Hudlicky, *Synlett* **2010**, 2701–2707.
[50] D. M. Zajonc, C. Cantu, J. Mattner, D. Zhou, P. B. Savage, A. Bendelac, I. A. Wilson, L. Teyton, *Nat. Immunol.* **2005**, *6*, 810–818.
[51] C. Rapp, C. Kalyanaraman, A. Schiffmiller, E. L. Schoenbrun, M. P. Jacobson, *J. Chem. Inform. Model.* **2011**, *51*, 2082–2089.
[52] S. Sirin, R. Kumar, C. Martinez, M. J. Karmilowicz, P. Ghosh, Y. A. Abramov, V. Martin, W. Sherman, *J. Chem. Inform. Model.* **2014**, *54*, 2334–2346.
[53] a) In *Prime, version 2021–2*, Schrödinger, New York, **2020**; b) J. L. Knight, G. Krilov, K. W. Borrelli, J. Williams, J. R. Gunn, A. Clowes, L. Cheng, R. A. Friesner, R. Abel, *J. Chem. Theory Comput.* **2014**, *10*, 3207–3220.
[54] S. Shah, M. Nagata, S. Yamasaki, S. J. Williams, *Chem. Commun.* **2016**, *52*, 10902–10905.
[55] a) T. Haifeng, Y. Yanghua, Y. Xinsheng, *Acad. J. Second Mil. Med. Univ.* **2002**, *23*, 246–249; b) H. Tang, Y. Yi, X. Yao, S. Zhang, Z. Xu, S. Mao, *Chin. J. Mar* **2003**, *22*, 8–12.
[56] V. Srikanth, R. Prasad, Y. Poornachandra, V. P. Babu, C. G. Kumar, B. Jagadeesh, R. C. R. Jala, *Eur. J. Med. Chem.* **2016**, *109*, 134–145.
[57] a) A. L. C. Isaad, P. Carrara, P. Stano, K. S. Krishnakumar, D. Lafont, A. Zamboulis, R. Buchet, D. Bouchu, F. Albrieux, P. Strazewski, *Org. Biomol. Chem.* **2014**, *12*, 6363–6373; b) A. Khan, F. Hollwedel, U. A. Maus, B. L. Stocker, M. S. M. Timmer, *Carbohydr. Res.* **2020**, *489*, 107951.
[58] E. Manzo, L. Fioretto, D. Pagano, G. Nuzzo, C. Gallo, R. De Palma, A. Fontana, *Mar. Drugs* **2017**, *15*, 288.
[59] S. Loya, V. Reshef, E. Mizrachi, C. Silberstein, Y. Rachamim, S. Carmeli, A. Hizi, *J. Nat. Prod.* **1998**, *61*, 891–895.

Manuscript received: July 2, 2022
Revised manuscript received: July 5, 2022
Accepted manuscript online: July 6, 2022
Version of record online: July 27, 2022